Check for updates

Coacervation for biomedical applications: innovations involving nucleic acids

Kimiasadat Mirlohi [ID] and Whitney C. Blocher McTigue [ID] *

Gene therapies, drug delivery systems, vaccines, and many other therapeutics, although seeing breakthroughs over the past few decades, still suffer from poor stability, biocompatibility, and targeting. Coacervation, a liquid–liquid phase separation phenomenon, is a pivotal technique increasingly employed to enhance the effectiveness of therapeutics. Through coacervation strategies, many current challenges in therapeutic formulations can be addressed due to the tunable nature of this technique. However, much remains to be explored to enhance these strategies further and scale them from the benchtop to industrial applications. In this review, we highlight the underlying mechanisms of coacervation, elucidating how factors such as pH, ionic strength, temperature, chirality, and charge patterning influence the formation of coacervates and the encapsulation of active ingredients. We then present a perspective on current strategies harnessing these systems, specifically for nucleic acid-based therapeutics. These include peptide-, protein-, and polymer-based approaches, nanocarriers, and hybrid methods, each offering unique advantages and challenges. Nucleic acid-based therapeutics are crucial for designing rapid responses to diseases, particularly in pandemics. While these exciting systems offer many advantages, they also present limitations and challenges which are explored in this work. Exploring coacervation in the biomedical frontier opens new avenues for innovative nucleic acid-based treatments, marking a significant stride towards advanced therapeutic solutions.

1. Introduction

Complex coacervation is a process of liquid–liquid phase separation that occurs in solutions of oppositely charged macromolecules,[1] such as proteins,[2] polysaccharides,[2] polynucleotides,[3] synthetic polymers,[4] surfactants,[5] and their combinations.[6–8] The driving force for coacervation is the electrostatic attraction between the charged groups of the macromolecules,[2,9,10] which is balanced by the entropic effects of the release of counterions and water molecules from the macromolecular complexes.[11–13] The resulting coacervate phase consists of microenvironments with a concentrated mixture of the interacting macromolecules without the need for membranes,[14] while the supernatant phase is depleted of them.[15,16] Coacervation was first observed by Bungenberg de Jong and Kruyt in the early 1900s in solutions of gelatin and gum arabic,[17] and since then it has been extensively studied and applied in various fields, such as food science,[18–21] personal care products,[22–24] biotechnology,[24,25] medicine,[26–29] and materials science.[26,30,31] Coacervation can be used to encapsulate, protect, and deliver biomolecules,[32,33] such as proteins,[34–37] enzymes,[7,38] and nucleic acids,[36,39–41] as well as

to create self-assembled structures, such as micelles,[38,42–44] vesicles,[45,46] and fibers.[47,48] The properties and applications of coacervates depend on the nature, composition, and ratio of the macromolecular components,[49–51] as well as on the environmental factors, such as salt concentration,[42,52,53] pH,[54–56] temperature,[57–59] and additives.[5,60,61]

In the biomedical field, coacervation is significant for its ability to encapsulate biomolecules, thereby enhancing their kinetic stability and delivery.[62] Encapsulation is particularly important for nucleic acid-based therapeutics, which are otherwise chemically unstable and vulnerable to enzymatic degradation[63] and have difficulties passively crossing the negatively charged biological membranes.[64] The importance of nucleic acid encapsulation extends beyond mere protection; it is a pivotal step in the stabilization of therapeutic molecules, which are often subject to the rigors of the cold supply chain.[65] The cold chain ensures precise temperature control to prevent degradation, which can significantly increase the cost and complexity of delivering these sensitive treatments, especially in resource-limited settings.[66] Coacervation-based encapsulation offers a promising avenue in this regard. By creating microenvironments that shield nucleic acids from thermal fluctuations and enzymatic activity, as well as allowing the potential for controlled release of the therapeutic cargo,[67,68] coacervation can potentially reduce or eliminate the need for

Department of Chemical and Biomolecular Engineering, Lehigh University, Bethlehem, PA 18015, USA. E-mail: whb322@lehigh.edu

cold chain logistics, thereby simplifying the distribution and storage of nucleic acid-based therapeutics. This could lead to more equitable healthcare delivery and a broader reach of life-saving treatments, particularly in areas where cold chain infrastructure is lacking or non-existent.

In this review, we provide a perspective on coacervation as a pivotal technique for nucleic acid delivery. We delve into the factors that influence coacervation processes and examine the various encapsulation methods that harness peptides, proteins, and polymers. The applications of coacervation in gene therapy, drug delivery systems, and vaccines will be highlighted, alongside a critical analysis of the challenges and limitations inherent to these approaches. Finally, we cast a forward-looking gaze at the future perspectives and research directions, discussing advanced coacervation techniques, targeted delivery systems, and the burgeoning potential of combination therapies. This review aims to provide a thorough understanding of the current landscape and the exciting possibilities in the realm of nucleic acid delivery.

2. Coacervation mechanisms and complex morphology

The complex coacervation process is a fascinating phenomenon predominantly occurring in colloidal systems, where two or more oppositely charged polymers interact in solution to form a dense, polymer-rich phase known as a coacervate, alongside a dilute polymer-poor phase referred to as the supernatant.[4] This phase separation is driven by electrostatic interactions between the charged groups of the polymers, leading to the aggregation and subsequent phase separation from the bulk solution. The mechanism behind complex coacervation involves a delicate balance of intermolecular forces, including electrostatic interactions, hydrogen bonding, and van der Waals forces, countered by the entropy-driven tendency of the system to remain mixed[4,69] (Fig. 1(A)). The entropic gains from the release of counterions are another significant driving force for phase separation.[70] In coacervation, while the oppositely charged polymers are aligning into condensates and therefore losing their local entropy, counterions are gaining their translational entropy by getting released into the supernatant.[70]

Depending on the structure and charge patterning of the polyelectrolytes within the system, various morphologies are possible for coacervates. A mixture of homopolymers leads to bulk phase separation.[42,67,71] The addition of a hydrophobic block to the polyelectrolyte can cause the formation of micelles with coacervate corona structures.[42,72] If hydrophilic but uncharged blocks (such as poly(ethylene glycol) (PEG)) are added to polyelectrolytes, coacervate-core micelles (C3Ms) become possible instead.[73–75] Hydrogel-like coacervate networks can be formed under higher concentrations of tri-block copolymers.[67,76,77] Although many complex morphologies are possible, here the structure and applications of bulk coacervate droplets, C3Ms, and coacervate-based hydrogels are highlighted (Fig. 1(B) and Table 1).

Bulk coacervate droplets are usually not stable structures for drug delivery as they coalesce after some time.[90,91] On the other
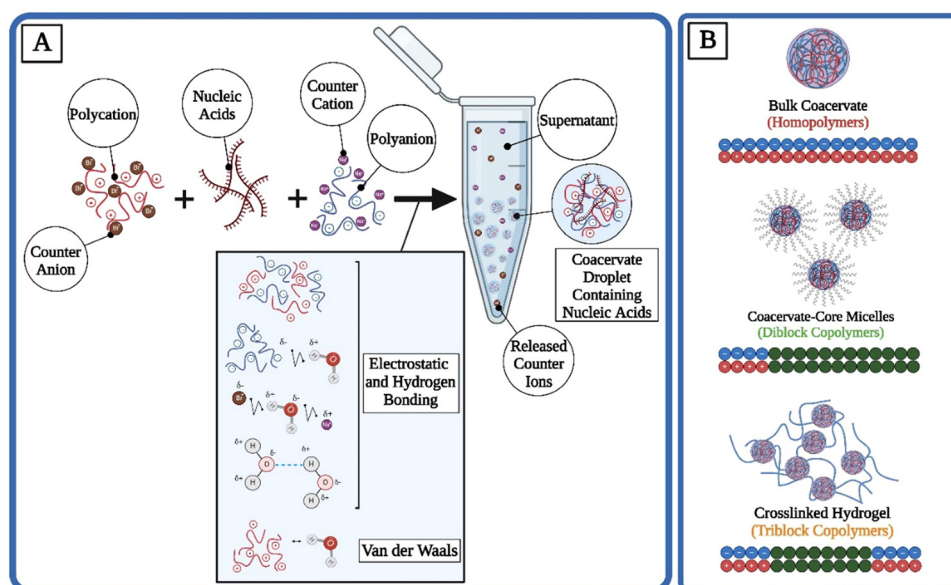

Fig. 1 Coacervation mechanisms and the effect of polymer structure on complex morphology. (A) In complex coacervation, polycations paired with negatively charged counter ions (*e.g.*, bromine) can interact with polyanions paired with positively charged counter ions (*e.g.*, sodium). Electrostatic interactions, hydrogen bonding, and van der Waals interactions are possible among all components within the aqueous solution. The dense coacervate droplets have high concentrations of the oppositely charged polyelectrolytes and encapsulate the nucleic acids, while the counter ions are released into the supernatant and help drive phase separation with the entropic gains of their release. (B) Homopolymers made of charged monomers form bulk complex coacervate droplets, di- and tri-block copolymers consisting of charged and uncharged sections can lead to coacervate-core micelles and crosslinked hydrogels, respectively (Created in BioRender. Mirlohi, K. (2024) **https://BioRender.com/l47c078**).

Table 1 Comparison of coacervation-based morphologies for biomedical applications. An overview of different coacervation-based morphologies, their polymer composition, biomedical applications, advantages, and disadvantages. This table highlights the versatility and challenges associated with bulk coacervates, coacervate-core micelles, and coacervate-based hydrogels in the context of nucleic acid delivery systems

Morphology	Polymers	Biomedical application example	Advantages	Disadvantages
Bulk coacervate	Homopolymers	Coating material for cell culture and biomimetic adhesives,[78] protocells,[79] bioimaging[80]	Simple preparation,[69] easier characterization[81]	Limited control over structure, the potential for coalescence, and instability[69]
Coacervate-core micelles	Di-block copolymers	Drug delivery, bioimaging[82]	High stability, therapeutically preferred size (10–100 nm),[83–85] promoted cellular uptake,[86] facilitated endosomal escape, tunable properties[86]	Challenging synthesis, the potential for aggregation[86]
Coacervate-based hydrogels	Tri-block copolymers	Tissue engineering,[87] wound healing[88]	High mechanical strength, flexibility, and tunable degradation rates[89]	Challenging crosslinking process,[87] potential for cytotoxicity[89]

hand, micelles, specifically polymeric micelles, are commonly employed structures as therapeutic carriers due to their stability in low concentrations, their clinically relevant size of 10–100 nm,[83] their ability to encapsulate and deliver hydrophobic drugs within their hydrophobic core, the opportunity to functionalize their surface for better targeting, and, lastly, their potential for concurrent delivery of multiple active ingredients[92] (Table 1). These versatile micelles can also incorporate coacervates within their core. For example, in a study by Vogelaar and coworkers, an antibiotic called colistin was complexed with poly(ethylene oxide)-*b*-poly(methacrylic acid) (PEO-*b*-PMAA) block copolymers to form C3Ms.[93] Colistin is used as a last resort treatment against Gram-negative bacterial infections, and their work showed decreased enzymatic degradation after complexation. Based on the entropy-driven mechanisms shown in Fig. 1, polymeric micelles can be prepared solely through the reduction of free energy.[92] However, it must not be concluded that enthalpy never plays a role. For example, under diluted conditions, polymeric micelles that have formed solely based on entropy gains can dissociate, making them unfit for parenteral (beyond intestinal) drug delivery applications.[92] Although isothermal titration calorimetry (ITC) measurements confirm that coacervation is not dominated by enthalpic effects, they confirm the experimental observations of enthalpy's role in coacervation: enthalpy has a small, positive contribution to coacervation.[70]

Lastly, coacervate-based hydrogel systems can be used for various drug delivery purposes where other methods might not be as effective, such as for oral ulcers. In their study, Chen and coworkers developed coacervate-based hydrogels composed of Pluronic F68 (F68) and tea polyphenols (TP) and reported that the F68-TP coacervates attached to porcine skin easily.[88] They demonstrated that their hydrogel system effectively addresses the issue of poor adhesion seen in conventional drug delivery systems within the moist environment of the mouth, while also accommodating the frequent movements of the lips. In summary, bulk coacervate droplets, micelles, and coacervate-based hydrogels each serve specific purposes in therapeutics. Bulk coacervates, while less structurally stable due to coalescence, are foundational in the study of phase separation. Polymeric micelles stand out for their stability, encapsulation capabilities, and potential for targeted delivery, making them invaluable for drug delivery applications. Lastly, coacervate-based hydrogels

are exceptionally suited for localized treatments like oral ulcers, offering improved adhesion and flexibility (Table 1).

3. Factors affecting coacervation

The formation of coacervates can be influenced by several factors essential to understanding the precise design and application of coacervate-based systems. Additionally, the ability to control phase behavior using a multitude of factors makes coacervation a wonderful technology for biomedical applications due to its tunability. Factors such as ionic strength, pH, temperature, and polymer structure and concentration play crucial roles in modulating coacervation.[94]

3.1 Environmental effects

3.1.1 Ionic strength. The ionic strength present in the solution is determined by the presence of charged species in the solution, which in turn controls the electrostatic interactions among the species involved in coacervation.[42,55] Critical salt concentration refers to the specific amount of added salt that prohibits phase separation.[95,96] Beyond this concentration, the electrostatic attraction between oppositely charged molecules is significantly reduced, leading to a decrease in coacervate yield.[97] Salt resistance is the ability of a coacervate system to maintain phase separation and stability despite increasing ionic strength.[14,98] For instance, in the coacervation of lactoferrin and β-lactoglobulin, no microscopic phase separation was observed beyond a salt concentration of 20 mM, and the coacervate yield decreased drastically with increasing NaCl concentration from 0 to 60 mM.[97] Similarly, the coacervation of hyaluronic acid and chitosan showed a strong dependence on ionic strength, with phase separation being almost unobservable at ionic strength ≥ 1.5 M NaCl.[99] Salt ions affect the coacervation of nucleic acids in various ways.[100] In their study, Onuchic and coworkers showed that an increase in the concentration of divalent Mg^{2+} reduces coacervation, demonstrated by a decrease in turbidity in systems of arginine-rich-peptide (RP3) and polyU (RP3-polyU).[101] They discuss that this agrees with their previous findings about monovalent (Na^+) cations which also reduce the propensity of phase separation, but divalent ions are more effective. Onuchic *et al.* studied other divalent cations such as Ca^{2+} and Sr^{2+}, both of which had lower

concentration thresholds required for phase separation. They argue that this might be due to the difference in charge density known to have extreme effects on RNA stability; for example, Ca^{2+} and Sr^{2+} better screen the charge of the phosphate backbone in RNA molecules and have weaker interactions with RNA compared to Mg^{2+}. Additionally, they showed that the RP3-polyU droplets become substantially more fluid as the concentration of Mg^{2+} increases from 0 mM to 100 mM.[101] Many groups have analyzed the effects of salt concentration on nucleic acid coacervates,[100–102] the more nuanced works of whom fall outside the scope of this paper. However, these findings highlight the critical role of ionic strength in modulating the formation and stability of coacervates in various systems.

3.1.2 **pH.** The pH affects the charge of the polymers involved, which in turn influences their interactions, the extent of coacervation, and the structure of the coacervate phase.[103] To study the intricacies of the effects of pH on polymer interactions, the acid dissociation constant (pK_a) and the isoelectric point (pI) of these molecules must be considered. The pK_a of a polymer determines the pH at which half of the molecules of that species are deprotonated.[104,105] It is a measure of the strength of an acid in solution. Lower pK_a values indicate stronger acids that donate protons more easily. At $pH < pK_a$, the group is protonated, whereas at $pH > pK_a$, the group would be deprotonated. The pI is the pH at which a molecule carries no net electrical charge, meaning that the negative and positive charges balance each other out. More explicitly, at $pH < pI$ the molecule carries a net positive charge, whereas at $pH > pI$ the molecule carries a net negative charge. Therefore, the pK_a and pI values must be accounted for to understand the extent and structure of the coacervate phase forming among polymers made up of ionizable groups.

For example, amino acids are weak polyelectrolytes known for the shift in their charge profile depending on the pH of their environment.[106–108] Amino acids have at least two pK_a values, one for the carboxyl group and one for the amino group, but they can have more pK_a values depending on their side chains. Therefore, pH controls the overall charge of peptides and polypeptides made of ionizable amino acids.[109] Similar principles apply to other polymers consisting of ionizable groups. For many systems, maximum electrostatic interactions and therefore coacervation are observed when the oppositely charged species have balanced charges, corresponding to charge neutralization.[9] This means that if two polymers with similar pK_a values are studied, they would achieve maximum complexation at balanced charges whereas with off-stoichiometric ratios, they would not experience the same extent of electrostatic affinity (Fig. 2(A)). To achieve both a balance of charges and more possible electrostatic interactions, an option is to use polymers with different pK_a values and conduct experiments at a pH away from both of their pK_a values, meaning that they would both be fully charged. For example, lysine, with a pK_a of approximately 11, and glutamate, with a pK_a of approximately 4, exhibit distinct ionization behaviors at physiological pH[110] (Fig. 2(B)). The Henderson–Hasselbalch equation elucidates that at pH values ~2 units away from pK_a, the charge of the amino acids will be close to ± 1.[109,111] At pH 7, lysine's amino group remains protonated, resulting in a positive charge, while glutamate's carboxyl group is deprotonated, giving it a negative charge. Consequently, homopolymers of lysine and glutamate would be fully charged at pH 7. This understanding is essential for predicting the electrostatic interactions and coacervation behavior of polypeptides, as the balanced charges at pH 7 lead to optimal conditions for coacervation.
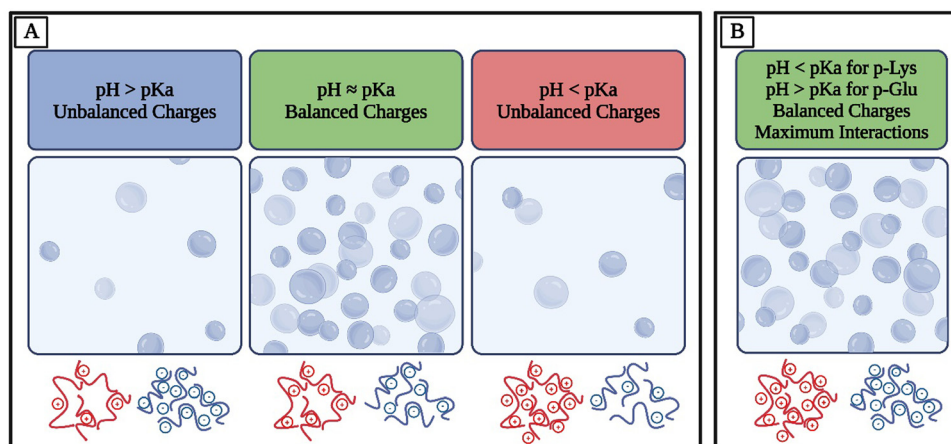

Fig. 2 A schematic demonstrating the effect of pH relative to pK_a and the balance of charges of the polymers present in the solution on phase separation. The charge density of polymers involved in coacervation depends on the pH relative to their specific pK_a values. (A) In the coacervation of polymers with similar pK_a values, as the pH approaches the pK_a of the polymers, their charges become more balanced, with nearly half of their ionizable charges protonated and the other deprotonated. While the polymers are not fully charged at this pH, their balanced charges improve their electrostatic interactions, consequently leading to phase separation. (B) In the coacervation of polymers with pK_a values further apart, the optimal pH for phase separation is away from the pK_a of both polymers. At this pH, they are both fully charged, and the opposite charges are also balanced, leading to an increase in electrostatic interactions. Schematics below each box illustrates relative charge of each species (Created in BioRender. Mirlohi, K. (2024) **https://BioRender.com/r80p465**).

Sensitivity to pH can allow control over the behavior of drug delivery systems that leverage coacervation, where they can release the cargo at specific pH ranges. For example, the targeted treatment of ulcerative colitis has been a challenge due to the wide pH range, and coacervate droplets containing emodin as the active ingredient have shown great promise due to their high stability and pH-responsive release behavior.[112] These concepts can be applied to the delivery of nucleic acids as well. In a study, Sun and coworkers designed histine-rich beak peptides (HB*pep*-K) that were redox- and pH-sensitive.[113] They were able to modulate the pH sensitivity of their peptide by conjugating the only lysine residue with a self-immolative moiety (HB*pep*-SR). At neutral pH, HB*pep*-K remains dissolved in the solution. However, when the sole lysine residue is modified with a self-immolative group, it can phase-separate into coacervates. In a reducing environment like the glutathione (GSH)-rich cytosol, HB*pep*-SR undergoes reduction, leading to self-catalytic removal of the SR group. This process causes the coacervate to disassemble. When HBpep-SR forms coacervates near neutral pH, it can encapsulate macromolecular therapeutics such as mRNA.[113] Upon exposure to cells, these therapeutic-loaded coacervates can cross the cell membrane through an energy-independent pathway, potentially involving cholesterol-dependent lipid rafts. Once inside the cytosol, the coacervates are reduced by GSH, leading to their disassembly and the release of the therapeutic agents. The pH-responsive behavior of coacervates can also help with modeling membrane-less organelles.[114,115]

3.1.3 Temperature.
Temperature is another environmental factor that can control phase separation. This is especially helpful considering that different sites in the body can have different temperatures. An example is the increased temperature at sites of inflammation, which means the possibility of controlled and more targeted release of cargo encapsulated within the coacervate phase.[116] It is also noteworthy that this process can be reversible with varying upper critical solution temperatures (UCST) and lower critical solution temperatures (LCST) in different systems.[99] The UCST is the temperature above which the components of a mixture are completely miscible in all proportions while the LCST is the temperature below which the components are completely miscible.[117] Hence, understanding the roles of UCST and LCST is crucial for designing any delivery system that may experience a temperature gradient to predict the formation or dissociation of the delivery system. Temperature has been employed as a control factor for the phase separation of nucleic acids in coacervates. For example, Deng and Huck encapsulated polyU and spermine coacervates with LCST ≈ 20 °C within liposomes and induced temperature change.[118] They showed that when the temperature was lower than the LCST, the coacervates gradually dissolved, whereas at a temperature above the LCST, a range of small coacervates formed which coalesced into a large coacervate over time. The fully reversible temperature-dependent behavior of these carriers is a look into their potential for biological compartmentalization. Deng and Huck also explored the incorporation of dsDNA molecules into the liposomes with

polyU/spermine complex coacervates and observed that at temperatures above LCST the dsDNA was encapsulated whereas when temperature dropped below the LCST, the dsDNA was released.[118] In addition to the nuanced roles that temperature plays in each specific system, temperature can also modulate the solubility and the molecular interactions of the polymers.[119] An increase in temperature can lead to enhanced molecular motion, potentially disrupting the coacervates, while a decrease may stabilize them by reducing thermal agitation.[120,121] The specific coacervate system must be studied to determine the precise effect of temperature on phase separation.

In addition to environmental factors such as pH and temperature affecting phase behavior, the characteristics of coacervate systems can be specifically chosen based on the desired application. The presence of salt ions in the solution affects the ionic strength of the system, and working with the temperature of the solution, they affect phase separation. Certain salts can increase the stability of polymers in the solution by enhancing their solubility which explains the thermo-responsive lower critical solution temperature (temperature below which the components of a mixture are completely miscible in all proportions) of such polymers.[119]

3.2 Polymer and system effects

The choice and design of monomers and the respective polymers involved in a system affects the possible and potential interactions within that system. For example, the concentration and properties of the present polymers play crucial roles. Polymer concentration determines the viscosity and the extent of the phase separation; higher concentrations favor coacervation by increasing the probability of intermolecular interactions.[122] Polymer structure, such as the chirality of monomers and charge patterning of the polymer, can determine the morphology and stability of the complexes formed in each system.[123] Charge patterning can dictate the phase behavior of coacervates and shift the binodal phase boundary, providing entropic advantages and influencing the thermodynamics of coacervation.[99] Chirality can influence biochemical interactions at a molecular level. In biomedical contexts, chirality can influence protein adsorption, cell adhesion, and subsequent behaviors which are crucial for the design of chiral biomaterials.[99] Chirality of polymers also affects the phase behavior of their mixture. Studies show that the presence of racemic polymers provides the opportunity for coacervation, whereas mixing homochiral polymers often yields precipitates and solid aggregates.[123–127]

The length and number of strands of the nucleic acid significantly influence phase separation, hence the stability and formation of coacervates.[128] Longer nucleic acids provide more binding sites for electrostatic interactions with the coacervate matrix, enhancing the stability of the encapsulated complex.[129] This increased interaction can lead to a more robust coacervate structure, capable of protecting the nucleic acid from degradation. Lebold and Best showed that phase separation is favored more in a 40-nucleotide ssDNA compared

to a 20-nucleotide ssDNA, and that this trend appears to hold for DNA lengths several orders of magnitude larger than the 20- and 40-nucleotide strands they used.[128] Additionally, Lebold and Best demonstrated that phase separation with dsDNA was favored over the more flexible ssDNA. Their results align with what Wand and coworkers noted in their work, where they found that coacervates composed of β-sheet poly(amino acid)s demonstrated greater protein encapsulation efficiency due to their reduced entropy and flexibility.[130] The work of Lebold and Best is investigated in more detail in Section 4.6, where the importance of their findings for hybrid systems that involve nucleic acids and other biomolecules is highlighted.

The sequence of nucleic acids can be pivotal for phase separation as it directly affects the electrostatic interactions based on the charge and polarity of the nucleotides, for example, guanine and cytosine have high charge densities. It is important to note that all the aforementioned factors play a role in the balance of electrostatic interactions, rather than having a clear and established role without any exceptions. To determine an outcome for specific systems, all species involved must be considered. For example, even though the charge density and secondary structure (when present) of nucleic acids seem like inherent factors in changing the encapsulation efficiency of a system, some studies suggest that it is much more complex than that. In their work, Frankel et al. compared an RNA sequence with no known secondary or tertiary structure (HH16 S) with another RNA sequence that has significant secondary structure (HDV E ribozyme).[131] They studied these oligonucleotides' ability to displace ATP in the coacervate phase with PAH and found that there was no apparent dependence on secondary structure. They argued that this could be explained by the strong affiliation of RNA nucleotides with PAH in coacervates due to their multivalency compared to ATP. This is just one example of how convoluted and intertwined factors affecting coacervation can be. To have clear and reliable sets of design rules for coacervate encapsulation systems for nucleic acids, much more research is required, both experimental and computational.

A critical decision in the design of encapsulation systems is the choice between binary and ternary systems. In binary systems, cargo, such as nucleic acids, serves as one of the phase-separating species. Conversely, in ternary systems, nucleic acids are sequestered within the coacervate phase through electrostatic interactions. Both binary and ternary coacervate systems offer distinct advantages. Binary systems are the most prevalent and their formation is more precisely regulated by the stoichiometry of the involved species, ionic strength of the solution (e.g., salt presence), and pH.[32,132,133] On the other hand, ternary systems made with polymers of similar length demonstrate higher salt resistance and can form over a wider range of polymer ratios compared to binary systems.[132,133] This increase in salt resistance and phase separation being possible at broader species ratios means environmental factors exert less influence on their formation, viscoelastic behavior, and stability.[32,132,134] A notable challenge for binary coacervate systems is that not all targeted cargo possesses sufficiently strong charges to bind effectively and remain associated with the oppositely charged species. Ternary systems, however, provide the capability to encapsulate even weakly charged cargo.[32,135] These systems are discussed further in Section 5.4.

In summary, the control of coacervation in biomedical applications hinges on a deep understanding of these factors. By manipulating pH, ionic strength, temperature, chirality, and charge patterning, researchers can design coacervate systems with desired properties for specific biomedical purposes. The interplay of these factors determines the efficiency and functionality of coacervates in various biomedical contexts. These parameters collectively dictate the physiochemical environment that governs coacervation. Adjusting these parameters can finely tune the formation, stability, and properties of the coacervates, making them suitable for various applications.[136]

4. Phase separation strategies involving nucleic acids

Understanding the behavior and properties of complex coacervates, especially those involving nucleic acids, sheds light on the fascinating world of intracellular organization and function, as well as developing therapeutics and drug delivery systems. The efficient delivery of nucleic acids to target cells in vivo presents a formidable challenge.[137,138] These molecules, crucial for gene therapy and other therapeutic applications,[63,139] face rapid degradation in biological media[140,141] and swift clearance from circulation.[138,142] To fully harness their therapeutic potential, they require sophisticated delivery systems that protect them, facilitate their transport to specific tissues, and ensure their functional integrity.

4.1 Incorporating peptides

Peptide-based coacervation relies on the self-assembly of peptides to form coacervates. This method benefits from the functional diversity of amino acids, allowing for the design of peptides with tailored phase separation properties and selective uptake of nucleic acids. In a study by Vieregg and coworkers, the interactions between DNA and polypeptides were explored.[143] They observed the effects of salt concentration and temperature on the phase separation of coacervate systems involving single-stranded DNA (ssDNA), double-stranded DNA (dsDNA), and poly(L-lysine) (pLys). They also experimented with the influence of the number of nucleotides (nt) and base pairs (bp) in their ssDNA and dsDNA respectively, as well as the number of amino acids in their pLys. Their studies showcase the tunability of peptide-nucleic acid coacervates comprehensively (Fig. 3).

The complex coacervation of dsDNA and polycations is less broadly studied due to precipitation, in contrast to the interactions between more flexible nucleic acids such as ssDNA and polycations which lead to liquid droplets (Fig. 3(A)). By exploring this less-studied case, Vieregg and coworkers showed that short dsDNA and pLys can escape precipitation.[143] For their
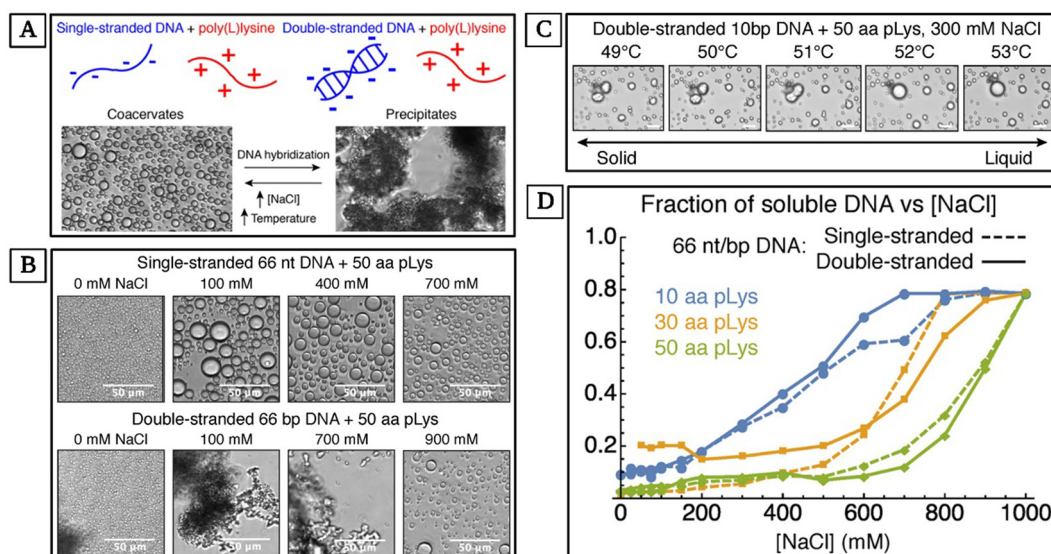
Fig. 3 Phase control of oligonucleotide−peptide complexes. (A) A summary of complex behavior based on the structure of DNA, concentration of salt, and temperature. (B) The effect of salt concentration on complexes between poly(L-lysine) (pLys) and 66 nt ssDNA, and pLys and 66 bp dsDNA. Oligonucleotides are released into the solution as the complex size decreases, but the loss during the precipitate–coacervate is small. (C) Complexes between 10 bp dsDNA and pLys at 300 mM NaCl. The mixture undergoes a melting transition at ∼51 °C. Solid complexes with round edges are observed just below this melting transition temperature and spherical liquids are observed at higher temperatures. (D) The change in the solubility of 66 nt/bp DNA when mixed with 10, 30, and 50 aa pLys, as NaCl concentration increases from 0 to 1000 mM. (Reproduced from ref. 143 with permission. Copyright 2018 American Chemical Society.)

observed complex phase diagram with liquid crystal (LC) meso-phases in bulk dsDNA, they argue that short dsDNA supramolecular aggregation and packing in the dense coacervate phase are the main phase behavior regulating parameters. Their work provides a deeper understanding of LC-coacervates which in turn may demystify structures and phase transition mechanisms in biomolecular condensates. Additionally, understanding these mechanisms can help with the design of stimuli-responsive synthetic self-assembled compartments, exploiting the prebiotic evolution of nucleic acids and peptides.[143] Vieregg et al. used bright-field and polarized transmitted optical microscopy to observe the phase behavior of a charge-balanced sample at different salt concentrations. At [NaCl] ≤ 700 mM, they only observed precipitate-like birefringent structures (Fig. 3(B)). At 800 mM ≤ [NaCl] ≤ 900 mM, fluid coacervate droplets formed (Fig. 3(B)). They showed the dehydration and rehydration of the coacervate LC mesophase transitions and observed the mixtures melting at ∼51 °C (Fig. 3(C)). Additionally, they studied the changes in the solubility of 66 nt ssDNA and 66 bp dsDNA complexed with 10, 30, and 50 amino acid pLys as they increased [NaCl] from 0 to 1000 mM. The transition to a single-phase state at higher salt concentrations was inconsistent for mixtures with ssDNA or dsDNA. However, for all systems, phase separation disappeared at NaCl concentrations of 1 M or higher, resulting in a uniform phase (Fig. 3(D)).

Coacervation has also been instrumental in advancing gene therapy by providing a means to protect and deliver genetic material effectively.[144,145] Peptide-based coacervates have been utilized for their high loading efficiency and excellent biocompatibility, which are essential for the delivery of therapeutic genes.[146,147] These coacervates facilitate the modulation of gene expression and have been applied in the treatment of various biological diseases.[146,148–151] The CRISPR gene therapy paradigm, in particular, has benefited from coacervation techniques, which have improved the delivery and stability of CRISPR/cas9 components, thus enhancing the precision and efficiency of gene editing[36] (Fig. 4). For example, Abbasi and coworkers were able to co-encapsulate Cas9 mRNA and guide RNA in coacervates for genome editing in mouse brain, demonstrating the potential of coacervation for in vivo genome editing.[152]

A recent study by Aman et al. demonstrated the use of gamma-modified peptide nucleic acids to facilitate targeted DNA invasion, showcasing the potential of peptide-based coacervation in gene editing technologies.[153] Aman and coworkers explored the integration of functional peptides into nucleic acid-based nanostructures and highlighted the enhanced biological activity and emerging properties achieved through their approach.[153] Their findings confirmed that T7 endonuclease I (T7EI, a structure-selective enzyme) can efficiently cleave DNA invaded by PNAs and demonstrated the potential of their system for targeted DNA cleavage.

4.2 Incorporating proteins

Protein-based coacervation is a nature-inspired approach for compartmentalization and protection of molecules such as nucleic acids. A factor making proteins great molecules for forming complex coacervates with nucleic acids is the diversity of possible interactions between these molecules.[154] In a study,
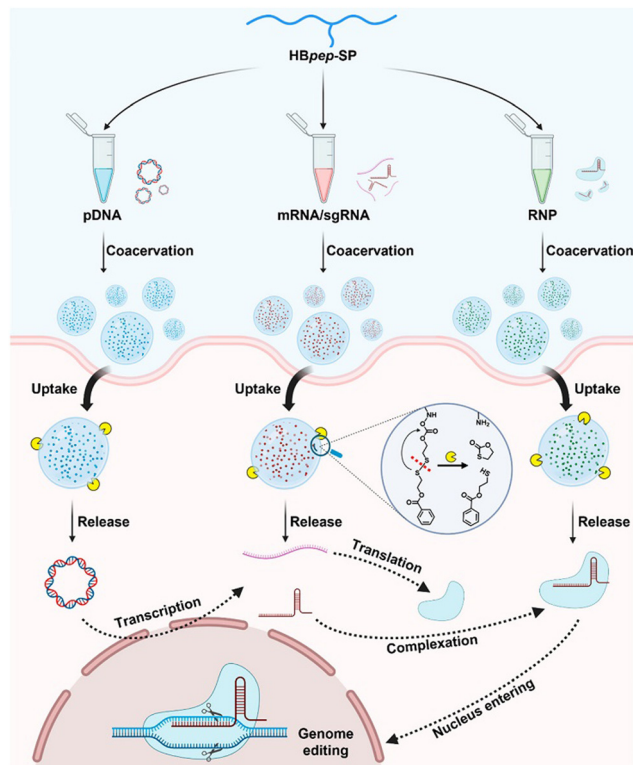
Fig. 4 Schematic presentation of universal delivery vehicle for CRISPR/Cas9 genome editing machineries. These machineries are mediated by a redox-responsive peptide (HBpep-SP) that undergoes LLPS due to changes in the pH. The coacervation, uptake, release, and genome editing mechanisms of plasmid DNA (pDNA), messenger RNA (mRNA), single guide RNA (sgRNA), and ribonucleoprotein (RNP) are shown (adapted from ref. 36 with permission. Copyright 2023 American Chemical Society).

Kaushik and coworkers examined the interpolymer interactions between elastin and DNA.[155] Interestingly, they found that complex coacervation was possible even when the concentrations of both elastin and DNA were extremely low (between 1 and 35 ppm). They argue that this phenomenon is explained by the ubiquity of DNA–protein interactions that can lead to self-assembled phases. This makes these systems extremely useful in biological applications, as high concentrations of biomolecules such as nucleic acids may not always be easily available.

In a study by Zhang and coworkers, the ability to store tau protein reversibly in complex coacervates with RNA was explored.[156] Tau is a neuronal protein that forms aggregates in the form of insoluble fibers through self-assembly in several neurodegenerative diseases such as Alzheimer's disease. Additionally, it was observed that in human neuronal cell culture, tau selectively binds to tRNA.[156] Zhang et al. discovered a state where many tau molecules maintain their solubility and native-like conformation in protein-rich coacervate droplets with RNA as the negatively charged constituent, which were shown to coalesce in vitro.[156] Their work demonstrated that tau-RNA droplets are responsive to changes in temperature and salt concentration. Consequently, these results showed the

physiochemical properties of tau that may cause it to have changes associated with neurodegenerative disease.

4.3 Incorporating polymers

Polymer-based coacervation involves the use of polymers to encapsulate nucleic acids, offering protection against enzymatic degradation and facilitating cellular uptake. The design of polymer-based nanoparticles has been a focus of recent research, aiming to ensure targeted delivery and controlled release of therapeutic nucleic acids.[100,157,158] Innovations in this field have led to the development of novel delivery systems for a broad range of infectious, chronic, and genetic disorders.[159–162]

Frankel et al. studied the complex coacervation of poly(allylamine hydrochloride) (PAH, 15 kDa) with anionic nucleotides adenosine 5′-mono-, di-, and triphosphate (AMP, ADP, ATP).[131] In their work, they explored the effect of PAH and nucleotide concentrations on the turbidity of solutions. They also measured turbidity as a function of PAH concentration with 2.5 mM ATP, 3.3 mM ADP, and 5 mM AMP (Fig. 5(I)). Additionally, they acquired optical micrographs of PAH/nucleotide coacervate droplets, where they mixed 38.5 μM PAH, 2 mM HEPES at pH 7, and with 5 mM Mg^{2+} (Fig. 5(II)). From their turbidity studies, they concluded that the coacervation between the nucleotides and PAH was maximal near charge neutralization which is consistent with previous studies.

The greater capacity of ATP and ADP to counteract PAH compared to AMP is evident in the broader range of PAH concentrations that exhibit liquid–liquid phase separation for the more strongly charged nucleotides.[131] When nucleotides were present at higher concentrations, samples sustained their turbidity at higher polyamine concentrations up to at least 100 μM PAH. Their work also suggested nucleotide self-association (Fig. 5(I)). They observed AMP-containing aggregates at 10 mM, which they argue might be due to poor packing of the solid particulates, which even after centrifugation did not show any compression (Fig. 5(II)).

A notable system that incorporates polymers in a coacervate delivery system is the use of chitosan, a natural biocompatible polysaccharide, to form DNA nanoparticles for oral allergen-gene immunization. In a study focused on peanut antigen-induced murine anaphylactic responses, Roy and coworkers showed that oral administration of chitosan–DNA nanoparticles led to gene expression in the intestinal epithelium.[163] Mice treated with nanoparticles containing a dominant peanut allergen gene (pCMVArah2) produced secretory IgA and serum IgG2a. Compared to non-immunized mice or those treated with naked DNA, the immunized mice exhibited a significant reduction in allergen-induced anaphylaxis, as evidenced by lower levels of IgE, plasma histamine, and vascular leakage. Their findings highlight the potential of polymer–DNA nanoparticles in modulating immune responses, especially notable for the biocompatibility of natural polymers such as chitosan.

In another study, Nishida and coworkers synthesized ligand-installed block copolymers for systematic delivery of siRNA,
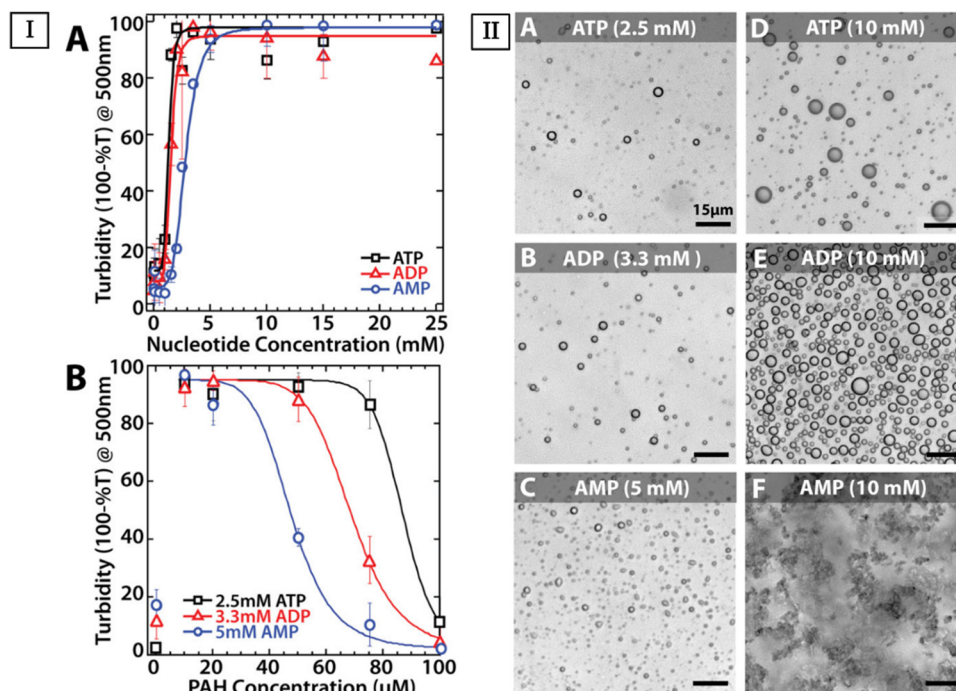
Fig. 5 Comparison of turbidity of solutions as a function of nucleotide and PAH concentration across different nucleotides, along with optical micrographs of these systems to highlight complex morphology. (I, A) Turbidity with 38.5 μM PAH as a function of nucleotide concentration. (I, B) Turbidity as a function of PAH concentration with 2.5 mM ATP (black squares), 3.3 mM ADP (red triangles), and 5 mM AMP (blue circles), all in 5 mM Mg^{2+} and 2 mM HEPES at pH 7. (II) Optical micrographs of PAH/nucleotide complexation prepared with 38.5 μM PAH, 2 mM HEPES pH 7, and 5 mM Mg^{2+}. (II, A–C) Solutions made with equal charge concentration of 10 mM negative and positive moieties with (A) ATP, (B) ADP, and (C) AMP. (II, D–F) The concentration of (D) ATP, (E) ADP, (F) and AMP were kept constant at 10 mM. Micrographs in II, A–E, show coacervation, while II, F shows an aggregate system. Scale bars represent 15 μm (Reproduced from ref. 131 with permission. Copyright 2016 American Chemical Society).

successfully silencing the E6 and E7 human papillomavirus (HPV) oncogenes.[164] They created micelles with ligand-installed, functionalized cRGD-PEG-PLK and siRNA, specifically designed to target the cancer cell surface. Their results from mice treated with these micelles for tumors demonstrated the great therapeutic potential of these systems against HPV-associated cancer. Other groups have incorporated uncharged functional polymers in poly-lysine/pDNA to make ternary complexes and achieved enhanced *in vitro* gene transfection without cytotoxicity, and take a step toward developing innovative gene and drug delivery systems.[165] In addition to delivery advantages provided by polymeric encapsulation systems for nucleic acids, some studies have focused on the potential of polymeric complexes in protecting nucleic acids and therapeutic proteins against freezing, heat, and freeze-drying stress.[166]

4.4 Nucleic acids in hybrid strategies and beyond

A great characteristic of coacervate encapsulation and delivery systems for nucleic acids is the ability to tune their properties by fine control over their structure and contents.[132,167] Therefore, it is possible to leverage the useful properties of various biomolecule groups at once, in the form of hybrid systems.

4.4.1 Nucleic acids as cargo. Nasr and coworkers designed nanocarriers to co-deliver mRNA (mCherry) and pDNA (pAmCyan1-C1, plasmid DNA encoding AmCyan fluorescent protein).[39] The pDNA they chose is based on gelatin type A

which is widely used in pharmaceutical applications for its biocompatibility and biodegradability. Additionally, they thermally stabilized their pDNA by the addition of gelatin to form a coacervate core in their nanocarriers. After designing these nanocarriers, Nasr *et al.* conducted cytotoxicity studies and observed that compared to untreated cells, murine dendritic cell line (DC2.4) cells treated with 340, 170, or 85 μg mL^{-1} particle concentration showed cell viability of 91.9%, 97.1%, and 97.7%, respectively, following 6 h incubation. They also did a 24 h incubation study with 170 μg mL^{-1} particle concentration which had 87.4% cell viability. Protamine-mRNA-pDNA CoAc assembled using 340, 170, 85 μg mL^{-1}, or 5-fold protamine doses showed no significant difference in cytotoxicity compared to P-TS-CoAc or untreated controls following 6 h incubation. 48 h post-treatment, their dual-loaded core–shell system had a transfection efficiency of 61.4 ± 21.6% for mRNA and 37.6 ± 19.45% for pDNA.[39] They report that the established commercial, experimental, and clinical reagents had failed, making their results a significant success. Considering the negligible cytotoxicity of their system, their findings provide insights into applications in vaccine formulations and other thermolabile therapeutics.

The surface charge of delivery vehicles plays an important role in cellular uptake and transfection efficiency.[168–170] To overcome this challenge, Li and coworkers proposed hybrid PEGylated nanoparticles (HNPs) in their study.[171] To provide

colloidal stability, they included an outer layer of poly(ethylene glycol) in the form of poly(ethylene glycol)-b-poly(aspartate)-adamantane (PEG-P(asp)-Ad). Their HNPs also included poly(ethyleminine)$_{10k}$ (PEI$_{10k}$) which forms complex coacervate with poly(asp) and prevents premature dissociation. Lastly, they decorated the PEI$_{10k}$ portion with cyclodextrin (PEI$_{10k}$-CD) to form the core with reporter plasmid DNA (pDNA). Their HNPs demonstrated enhanced *in vitro* transfection and increased stability compared to traditional PEGylated nanoparticles (PEG-NP). Their study of intratumoral injections compared the delivery efficiencies of HNPs, PEG-NP, and PEI$_{25k}$, and highlighted the success of HNPs in delivering pDNA into tumors. They argue that this enhanced efficiency is a result of the PEG shell and coacervation integration at the interface of PEI$_{10k}$-CD/pDNA core compared to PEG-NP and PEI$_{25k}$.

In another study, Cai *et al.* studied coacervate systems involving gold nanoparticles (AuNPs) functionalized with elastin-like peptides (ELPs) as potential delivery systems.[172] Their AuNPs were functionalized with a cysteine-terminated 96-repeat of the VPGCG sequence (V96-Cys). ELPs are known to be thermo-responsive,[173] which allowed for controlling the size of these particles from 250 to 930 nm.[172] Their findings were that ELP-decorated AuNPs form clusters in a coacervate phase in the presence of free unimers (single chains of V96-Cys) above the transition temperature (T_t). These clusters in the coacervate phase can then release their entrapped cargos below T_t.[172] They demonstrated the possibility of precise control over the amounts of hydrophobic molecular cargos, specifically the dye Nile red (NR) and tetracycline (TC) which is a broad-spectrum antibiotic, encapsulated during coacervation, and subsequently released below T_t during deconstruction. As predicted, Cai and coworkers observed the inhibition of cell growth with increased cluster size.

The hydrophobicity of TC is specifically important as their enhanced bioavailability is explored.[172] Their results show an avenue for rapidly releasing precise amounts of cargo from size-controlled clusters in the coacervate phase, in addition to being responsive to environmental factors. This can have remarkable applications in drug delivery, combination photothermal therapy, and theranostic applications.[172] The creative approach to nucleic acids as functionalizing groups rather than cargo itself brings about even more opportunities to leverage various properties of these biomolecules.

4.4.2 Nucleic acids beyond cargo. Many encapsulation systems for nucleic acid delivery use tertiary systems, where two polymers form a coacervate phase which encapsulates the nucleic acid as the cargo. However, it is also possible to have nucleic acids as the coacervating polymers themselves. Using a minimal coarse-grained model, Lebold and Best showed coacervates are readily formed at physiological ionic strengths in a prototypical mixture of nucleic acids with the polycationic C-terminus of histone H1 (CH1).[128] Their results show an increase in local ordering at low ionic strengths. Additionally, they showed that for well-mixed or moderately blocky distributions of charge, local ordering moderately increases with increasing blockiness also associated with an increased

propensity to phase separate. They explain that although this ordering is associated with a slowdown of rotational and translational diffusion in the dense phase, for more extreme blockiness and higher local charge density, a qualitative change in the condensed phase is observed due to a dramatic increase in the ordering of the DNA.

The findings of Lebold and Best regarding the formation of coacervates in mixtures of nucleic acids and histones agree with experimental results. Leicher and coworkers explored the binding and coacervation of nucleic acids by linker histone H1.[174] Their work provides a more nuanced perspective on what role H1 plays in genome organization and maintenance while providing insight into the effects of single- or double-strandedness of nucleic acids on how they interact with H1 and their assembly dynamics. They found that ssDNA has a higher absorbance index compared to dsDNA, indicating more complexation (Fig. 6(A) and (B)). Additionally, they investigated the effect of the size of the nucleic acid chain on absorbance for the mixture of H1 with ssDNA, dsDNA, and RNA (Fig. 6(C)–(E)). They found that longer chains of ssDNA yield higher turbidity readings when complexing with H1 (Fig. 6(C)) and confirmed that ssDNA has higher turbidity values compared to dsDNA with the same sequence and length (Fig. 6(D)). Additionally, they observed the same pattern of increasing turbidity values with increasing length when studying RNA mixtures with H1 instead of ssDNA and dsDNA (Fig. 6(E)).

4.4.3 Membrane-less organelles. As discussed earlier, an innovative approach to modeling membrane-less organelles is studying the dynamics of coacervation.[115,175–177] To do so, Aumiller and coworkers designed RNA-based coacervates to understand the phase separation responsible for the formation of P granules, nucleoli, and other membrane-less subcellular compartments composed of RNA and proteins.[178] In their study, they showed that low-complexity RNA (polyuridylic acid, polyU) and short polyamines (spermine and spermidine) are similar in many ways to coacervates involving intrinsically disordered proteins (IDPs). These polyU/polyamine coacervates compartmentalize biomolecules in a sequence- and length-dependent manner (Fig. 7(A) and (B)). The significance of these findings is highlighted by the reversibility of coacervation based on changes in temperature as the structure of polyU which impacts its interactions with polyamines (Fig. 7(C)). Additionally, they showed that these biomolecules maintain their mobility within the coacervate droplets (Fig. 7(D)). Lastly, Aumiller *et al.* conducted a FRAP analysis of the poly U15 and demonstrated that lipid vesicles assemble at the interface of the coacervate phase without impeding RNA entry/egress (Fig. 7(E)). These vesicles maintain their integrity at the interface and can go through temperature-induced droplet dissolution.

A step forward beyond modeling membrane-less organelles in biological systems is using these structures to manipulate life processes.[177] In an effort toward this goal, Zhang and coworkers designed photoactivatable DNA membrane-less organelles using coacervation that were self-stabilizing.[177] Specifically, they generated long single-stranded DNA *via* rolling circle amplification (RCA, an enzymatic process used to amplify
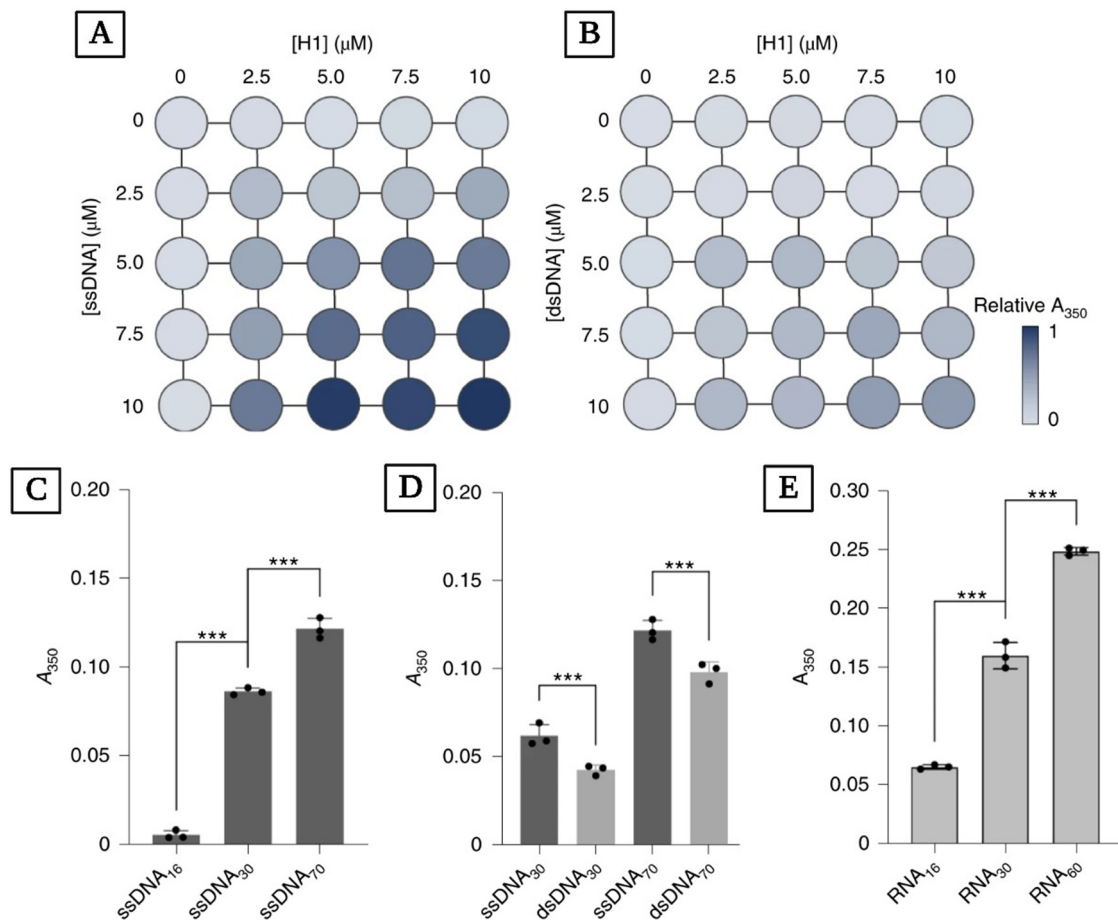
Fig. 6 Studying the complexation of H1 with ssDNA, dsDNA, RNA, and the effects of nucleic acid length on the turbidity of these mixtures. Matrix representation of turbidity (A_{350}) measured at different concentrations of H1 and ssDNA (A) and dsDNA (B). (C) Turbidity readings for mixtures of full-length H1 with ssDNA of different lengths. ssDNA concentrations were normalized to yield the same total number of nucleotides (44 µM $ssDNA_{16}$, 23 µM $ssDNA_{30}$, 10 µM $ssDNA_{70}$). (D) Turbidity values for H1 mixed with ssDNA and dsDNA of the same length and sequence. The concentrations of nucleic acids were normalized to yield the same number of nucleotides (10 µM $ssDNA_{30}$/5 µM $dsDNA_{30}$ and 10 µM $ssDNA_{70}$/5 µM $dsDNA_{70}$). (E) Turbidity values for H1 mixed with different lengths of RNA. RNA concentrations were normalized to yield the same number of nucleotides (44 µM RNA_{16}, 23 µM RNA_{30}, 12 µM RNA_{60}). ***$P < 0.001$ using one-way analysis of variance (ANOVA) with Tukey's test for multiple comparisons (reproduced from ref. 174 with permission. Copyright 2022 Nature).

circular DNA or RNA molecules[179]) and used it as the scaffold assembling into membrane-less coacervates. Their DNA membrane-less organelles recruited RCA byproducts and other components which provided for their self-stabilization. Additionally, their condensation had the desired nanoscale size of 10–100 nm.[83,177] Their photoactivatable DNA membrane-less organelles accumulated and managed cancer in a mouse model in a spatiotemporal manner. Their results are promising for designing highly stable DNA coacervate membrane-less organelles with controllable bioactivity. This advancement paves the way for developing even more intricate coacervate nucleic acid systems capable of executing sophisticated tasks and regulating complex life processes.

5. Challenges and future explorations

5.1 Stability and delivery

The burgeoning field of coacervation-based delivery systems for nucleic acids is not without its challenges and limitations.

Stability issues are at the forefront, as the integrity of coacervates is paramount for the effective delivery of nucleic acids. The lack of a physical membrane in bulk coacervates can lead to rapid coalescence or collapse of the coacervate phases, compromising their structural integrity.[180,181] Some methods have been explored to mitigate this challenge. For example, incorporating comb polyelectrolytes in complex coacervates has shown promise in stabilizing phase separation.[181] Other groups have explored the effects of mixing flow conditions and polymer composition on coalescence, sedimentation, and aggregation in coacervate systems.[182] However, more systematic studies are necessary to formulate the specific factors and their boundaries within coacervate systems for controlling and maintaining phase separation. Another avenue to explore for mitigating the structural maintenance issues is to use di- and tri-block copolymers that are capable of forming more complex and stable structures and systems such as micelles and hydrogels.[86]

Maintaining stability in the complex biological milieu also remains challenging due to factors like pH, salt concentration,
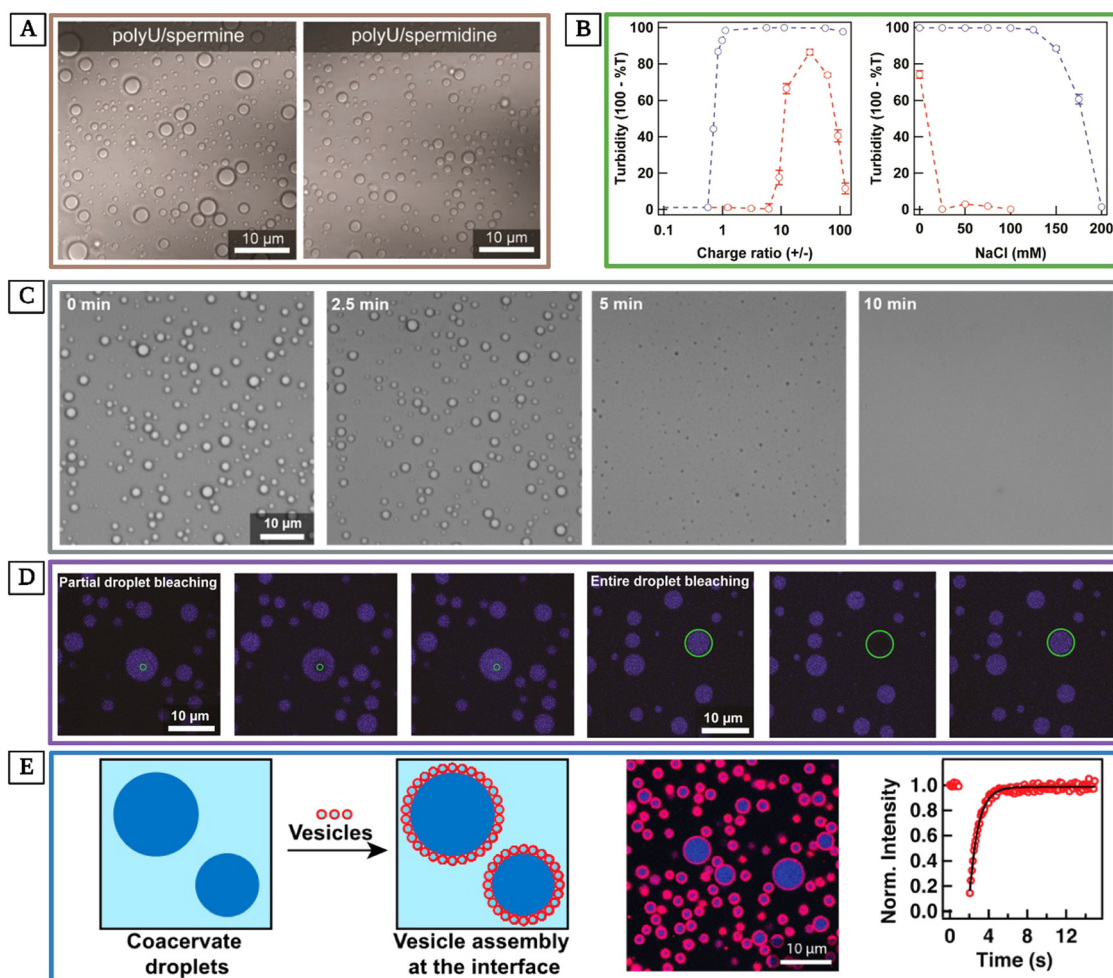
Fig. 7 Exploring RNA-based coacervates as models for membrane-less organelles. (A) Transmitted light differential interference contrast (DIC) micrographs of bulk polyU/spermine (0.05% polyU and 0.05% spermine weight percent, a charge ratio of 56 : 1) and polyU/spermidine (0.05% polyU and 0.05% spermidine weight percent, a charge ratio of 61 : 1). (B, left) Turbidity values *versus* charge ratio for polyU complexing with spermine (blue) and spermidine (red). (B, right) Turbidity values for 0.05% polyU complexing with 0.5% spermine (blue) or 0.5% spermidine (red) *versus* 25 mM NaCl concentration at 37 °C. (C) Images of polyU/spermine coacervate dissociation after incubation at 37 °C for 30 min and gradual decrease in temperature starting at $t = 0$ at a rate of 10 °C min^{-1} to 10 °C. Droplets are almost completely dissolved after 5 min, and they are fully dissociated after 10 min. Concentrations were 0.05% polyU and 0.5% spermine (a charge ratio of 56 : 1) or 0.5% spermidine (a charge ratio of 61 : 1). (D) The partial and entire droplet bleaching studies demonstrate rapid recovery, showcasing the retaining of solute mobility within the coacervate droplets. (E, left) Schematic showing the assembly of lipid vesicles (red circles, not drawn to scale to show individual vesicles) around polyU/spermine coacervates (blue circles). (E, right) DIC and confocal fluorescence images of the polyU/spermine droplets containing fluorescent poly U15, as well as FRAP recovery curve of entire droplet bleaching of the Alexa Fluor 647 poly U15. All scale bars represent 10 μm (reproduced from ref. 178 with permission. Copyright 2016 American Chemical Society).

and temperature variations.[183,184] Additionally, the encapsulated nucleic acids must be protected from enzymatic degradation by nucleases, which is a significant hurdle. While coacervation can enhance the stability of encapsulated cargos, their stability in blood and other biological fluids during storage and upon administration remains a concern.[83] Current therapeutics involving nucleic acids would immensely benefit from enhanced kinetic stability, which would increase their shelf life.[136] Controlled and sustained release of nucleic acids is also crucial for therapeutic efficacy. The dynamic nature of the biological environment, including interactions with proteins and other biomolecules, can significantly affect release rates.

Achieving precise control over release kinetics is complicated by the need to balance stability and permeability.[185] Some groups have explored the effects of coacervating species or additives on better control over the release kinetics. For example, Ardestani and coworkers characterized caseinate–pectin coacervates as delivery systems for saffron extract.[186] They argued that core/shell and protein/polysaccharide ratios play crucial roles in encapsulation efficiency and loading capacity. Additionally, they argued that the presence of the "guest molecule", saffron extract, resulted in higher rheological moduli, therefore enhancing thermal, structural, and microstructural properties of the coacervates.[186] An area of research in

need of further exploration is the effects of additives or "guest molecules" on the properties of coacervates incorporating nucleic acids. Recent studies have utilized molecular dynamics and machine learning to better understand and optimize these mechanisms, however, the variability in biological conditions still poses a significant challenge.[7,130]

5.2 Immunogenicity and clinical life cycle

Ensuring biocompatibility is essential to avoid adverse immune responses. While coacervates can be formulated from biocompatible materials and even decrease the cytotoxicity of what they're encapsulating,[187] their interaction with cells and tissues must be carefully evaluated to prevent cytotoxicity and immunogenicity.[188] The potential for unintended interactions with cellular components can lead to adverse effects, necessitating thorough preclinical testing.[146] For example, although poly-lysine has been commonly studied in coacervates for years and has shown great promise,[34,189,190] it can cause cytotoxicity at high concentrations.[191] Therefore, all coacervate systems must be carefully tested from different perspectives to ensure their safety. Additionally, the scalability and reproducibility of coacervate formulations for clinical applications remain areas of active research. Some significant challenges include manufacturing, as the complexity of coacervate systems can make large-scale production difficult. Ensuring consistent quality and performance across batches is critical for clinical translation. Efficient delivery to target cells and tissues requires overcoming biological barriers such as cellular uptake and endosomal escape. Strategies like surface modification with targeting ligands are being explored to enhance specificity and efficacy,[192] but much more enhancement is yet to be achieved.

5.3 Further avenues

The landscape of coacervation in nucleic acid delivery is poised for significant advancements, with research efforts converging on the development of advanced coacervation techniques. These novel approaches aim to refine the encapsulation process, enhance the stability of coacervates, and improve the precision of delivery.

5.3.1 Targeted release.
Targeted delivery systems represent another frontier in coacervation research, and much has been accomplished, especially in applications of cancer treatment and gene delivery.[149,193–195] Targeted delivery of therapeutics in coacervates has also been promising for gene editing.[152] The goal of targeted release is to achieve site-specific delivery of nucleic acids, maximizing specificity, minimizing off-target effects, and improving therapeutic efficacy. Peptide-enabled targeted delivery systems, in particular, have garnered attention for their ability to improve binding specificity and effective accumulation of drugs at the site of interest.[146,196] It is possible to use these peptides in coacervate systems to improve targeting. The potential of combination therapies is also being explored in conjunction with coacervation techniques.[197] In a study for liver cancer treatment, Lin and coworkers developed nanoreactor coacervates that showed remarkable effectiveness against tumors by triggering ferroptosis and apoptosis in

tumors, while aiding in the activation of an adaptive T-cell response which further curbs the growth of distant tumors *in vivo*.[197] The synergy between coacervate-based delivery systems and other therapeutic modalities could lead to more effective treatments for complex diseases. Precision combination therapies tailored to specific oncogenic alterations are a potential example of how coacervation could be integrated into a multifaceted treatment approach, offering a comprehensive resource for targeted therapeutic interventions.[198] Incorporating nucleic acids into these strategies could further enhance the precision and efficacy of targeted therapeutic interventions, opening new avenues for advanced medical treatments.

5.3.2 Lipid nanoparticle hybrid systems.
Lipid nanoparticles (LNPs) are renowned for their superior structural stability, which can significantly improve the overall stability of coacervate systems.[199–201] While LNPs have shown great promise in nucleic acid delivery, their low nucleic acid loading capacity could potentially be enhanced by incorporating the electrostatic interactions that coacervation offers.[199] A less explored class of hybrid systems for nucleic acid delivery using coacervation includes those incorporating lipids.[3,202] The structural stability provided by lipids, combined with the robustness contributed by polymers that may be used in the coacervate phase, could allow for better control over nucleic acid loading and release kinetics.[40,199] Additionally, a recognized issue for nanoparticles is the formation of a protein corona once they enter the bloodstream, which facilitates recognition by phagocytic cells and subsequent clearance from the body, while also inhibiting the ligands on the nanoparticle surface responsible for active targeting.[203] Research shows that the addition of a polyethylene glycol (PEG) corona to these nanoparticles can prevent protein corona formation and reduce nanoparticle clearance from the body.[203,204] There is substantial potential in designing delivery systems that combine the benefits of multiple macromolecule groups and mechanisms, such as incorporating lipids, polymers, proteins, and coacervation in a single hybrid system. However, these designs would be extremely complex and difficult to consistently produce. Despite the potential advantages, there are limited studies exploring existing hybrid systems, making the design of even more intricate ones a challenge. The next step for current hybrid systems would be more comprehensive cellular assessments to understand their interactions, nucleic acid loading, and delivery efficacy, leading to a clearer picture of the role these hybrid systems can play in therapeutic applications and their clinical translation.

5.4 Looking onward

The regulatory landscape for nucleic acid-based therapeutics is still evolving. Ensuring compliance with regulatory standards for safety, efficacy, and quality is essential for successful clinical translation. Moreover, there is a need for more explicit experimental exploration of nucleic acids within coacervates. Studies have shown that coacervates can effectively encapsulate and protect nucleic acids, but detailed experimental

investigations are required to fully understand the dynamics and interactions within these systems.[91] The species involved in coacervation, and their charges greatly influence these systems, as discussed earlier. Whether binary or ternary systems are more effective for nucleic acid delivery, and the charge composition of these molecules for optimal encapsulation and protection against environmental factors and nucleases, require further investigation. For instance, studies have demonstrated enhanced protection of nucleic acids against nucleases when encapsulated within a thermally stabilized coacervate core nanocarrier.[39] Moreover, ternary coacervate systems of synthetic polymers have shown greater stability against environmental changes compared to binary systems.[132] Combining these findings in a comprehensive study of nucleic acid stability against environmental changes and nucleases could allow us to compare the performance of binary and ternary coacervate systems for nucleic acid delivery.

Additionally, understanding the optimal charge composition in ternary systems is essential. Ternary systems with oppositely charged molecules can help encapsulate weakly charged cargos,[32,135] raising questions about the behavior of strongly charged molecules within ternary combinations, such as nucleic acids. A ternary system would enhance crowding effects by increasing the number of species involved and provide greater versatility in system properties.[15,16,205] However, if another negatively charged molecule is present alongside nucleic acids, it could compete for interactions with positively charged species, potentially increasing the number of free nucleic acid molecules within the system with reduced stability. On the other hand, incorporating two different positively charged molecules could increase electrostatic interaction involving nucleic acids. This approach has been previously applied to nucleic acid aggregates[206] and systems without nucleic acids,[132] and a comprehensive study applying these insights to nucleic acid encapsulation systems would be highly beneficial. A further necessary consideration is for the interactions of nucleases with each present species. Coacervate systems have been explored as a means to enhance the catalytic activities of enzymes,[207,208] which raises questions about design rules that prevent this enhanced enzyme activity when encapsulating nucleic acids to protect them against nucleases.

Recent research has highlighted the potential of peptide-based coacervates as biomimetic protocells, which can sequester and concentrate a wide range of solutes, including nucleic acids.[102] These coacervates offer a versatile platform for studying the phase separation and selective uptake of guest molecules, which is crucial for optimizing their use in therapeutic applications.[102] Future investigations employing cellular assays can provide insights into cellular uptake, intracellular trafficking, and the overall therapeutic efficacy of the delivery systems.[83,209] High-throughput screening platforms, such as RNA-encoded peptide barcodes, have been developed to evaluate the functional delivery of lipid nanoparticles *in vivo*, which can accelerate the discovery of new technologies for mRNA delivery.[209] Additionally, polymeric micelle-based delivery systems have shown promise in enhancing the stability and

cellular uptake of nucleic acids, addressing key challenges in their clinical translation.[83] These advancements underscore the importance of continued research and innovation in the field to achieve safe and effective nucleic acid-based therapeutics.

6. Conclusion

Coacervation is an innovative mechanism employed in numerous nucleic acid delivery systems for a variety of biomedical applications, including drug delivery and gene therapy. Various factors such as pH, ionic strength, temperature, polymer concentration and structure, the length and sequence of the encapsulated nucleic acids, and the number of species involved in complexation significantly influence and control coacervation-based nucleic acid encapsulation systems. These numerous controlling factors render these encapsulation systems highly tunable, allowing for precise manipulation of the properties of the constituent species and the environmental conditions. However, the necessity to consider such a multitude of factors, coupled with the complexities of the biological milieu and potential immune responses elicited by these delivery vehicles, presents significant challenges for their practical application and large-scale production.

Stability issues of the encapsulated nucleic acids and the coacervate phase itself remain a critical concern. The lack of a physical membrane can lead to coalescence or collapse of the coacervate phase, compromising the structural integrity of delivery systems. Additionally, our understanding of the loading and release kinetics of nucleic acids within coacervate systems is still incomplete, complicating the optimization of these delivery vehicles for therapeutic use.

Moreover, there remains a substantial gap in our understanding of coacervate-based encapsulation systems for nucleic acid delivery, particularly regarding their interactions with cells and the body as a whole. This gap encompasses several critical aspects, including the mechanisms by which coacervates interact with cellular membranes, the intracellular trafficking pathways they utilize, and their potential immunogenicity. Understanding these interactions is crucial for optimizing the design of coacervate-based delivery systems to ensure efficient and targeted delivery of nucleic acids while minimizing adverse effects.

Future research should continue to explore hybrid systems that incorporate various materials such as peptides, polymers, proteins, and lipids to harness their combined advantages. For instance, incorporating peptides can enhance cell penetration and targeting, while polymers can provide structural stability and controlled release properties. Proteins can offer specific binding capabilities, and lipids can improve membrane fusion. Such hybrid systems could significantly advance our understanding of the dynamics within these nucleic acid encapsulation systems, leading to more effective and versatile delivery platforms. Additionally, comprehensive cellular assays including studies on cellular uptake, intracellular trafficking, release kinetics, and the biological activity of the delivered nucleic
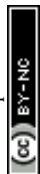
acids are essential to elucidate the cellular interactions and efficacy of nucleic acid loading and delivery, ultimately paving the way for therapeutic applications and clinical translation.

Data availability

No primary research results, software or code have been included and no new data were generated or analyzed as part of this review.

Conflicts of interest

There are no conflicts to declare.

References

1 A. N. Singh and A. Yethiraj, *J. Phys. Chem. B*, 2021, **125**, 3023–3031.

2 C. G. De Kruif, F. Weinbreck and R. De Vries, *Curr. Opin. Colloid Interface Sci.*, 2004, **9**, 340–349.

3 J. R. Vieregg and T.-Y. D. Tang, *Curr. Opin. Colloid Interface Sci.*, 2016, **26**, 50–57.

4 C. E. Sing and S. L. Perry, *Soft Matter*, 2020, **16**, 2885–2914.

5 W. Zhao and Y. Wang, *Adv. Colloid Interface Sci.*, 2017, **239**, 199–212.

6 T. P. Fraccia and N. Martin, *Nat. Commun.*, 2023, **14**, 2606.

7 J. Zheng, P. Van der Meeren and W. Sun, *Aggregate*, 2024, **5**, e449.

8 N. Khan and B. Brettmann, *Polymers*, 2019, **11**, 51.

9 E. Kizilay, A. B. Kayitmazer and P. L. Dubin, *Adv. Colloid Interface Sci.*, 2011, **167**, 24–37.

10 S. Chen and Z.-G. Wang, *Proc. Natl. Acad. Sci. U. S. A.*, 2022, **119**, e2209975119.

11 Z. Ou and M. Muthukumar, *J. Chem. Phys.*, 2006, **124**, 154902.

12 X. Xu, Q. Ran, P. Dey, R. Nikam, R. Haag, M. Ballauff and J. Dzubiella, *Biomacromolecules*, 2018, **19**, 409–416.

13 M. Ghasemi, S. Friedowitz and R. G. Larson, *Soft Matter*, 2020, **16**, 10640–10656.

14 A. Sathyavageeswaran, J. Bonesso Sabadini and S. L. Perry, *Acc. Chem. Res.*, 2024, **57**, 386–398.

15 S. Biswas, A. L. Hecht, S. A. Noble, Q. Huang, R. E. Gillilan and A. Y. Xu, *Biomacromolecules*, 2023, **24**, 4771–4782.

16 A. M. Marianelli, B. M. Miller and C. D. Keating, *Soft Matter*, 2018, **14**, 368–378.

17 P. Koets, *J. Phys. Chem.*, 1936, **40**, 1191–1200.

18 T. Moschakis and C. G. Biliaderis, *Curr. Opin. Colloid Interface Sci.*, 2017, **28**, 96–109.

19 L. A. Bosnea, T. Moschakis and C. G. Biliaderis, *Food Bioprocess Technol.*, 2014, **7**, 2767–2781.

20 B. Wu, B. Degner and D. J. McClements, *J. Phys.: Condens. Matter*, 2014, **26**, 464104.

21 S. Rojas-Moreno, F. Cárdenas-Bailón, G. Osorio-Revilla, T. Gallardo-Velázquez and J. Proal-Nájera, *Food Measure*, 2018, **12**, 650–660.

22 A. Ammala, *Int. J. Cosmet. Sci.*, 2013, **35**, 113–124.

23 C. Lepilleur, J. Mullay and C. Kyler, *J. Cosmet. Sci.*, 2011, **62**, 161–177.

24 J. D. Tang, S. R. Caliari and K. J. Lampe, *Biomacromolecules*, 2018, **19**, 3925–3935.

25 D. Magnin, *Carbohydr. Polym.*, 2004, **55**, 437–453.

26 W. C. Blocher and S. L. Perry, *Wiley Interdiscip. Rev.: Nanomed. Nanobiotechnol.*, 2017, **9**, e1442.

27 Ö. Karabıyık Acar, S. Bedir, A. B. Kayitmazer and G. T. Kose, *Int. J. Biol. Macromol.*, 2021, **188**, 300–312.

28 K. O. Margossian, M. U. Brown, T. Emrick and M. Muthukumar, *Nat. Commun.*, 2022, **13**, 2250.

29 J. George Joy, H. K. Son, S.-J. Lee and J.-C. Kim, *J. Ind. Eng. Chem.*, 2024, **134**, 432–447.

30 Y. Hong, S. Yoo, J. Han, J. Kim, Y. Lee, Y. Jho, Y. S. Kim and D. S. Hwang, *Commun. Chem.*, 2024, **7**, 1–10.

31 M. Li, R. Mirshafian, J. Wang, H. Mohanram, K. A. Ahn, S. Hosseinzadeh, K. V. Pervushin, J. H. Waite and J. Yu, *Biomacromolecules*, 2023, **24**, 4190–4198.

32 E. Ban and A. Kim, *Int. J. Pharm.*, 2022, **624**, 122058.

33 T. Lu, X. Hu, M. H. I. van Haren, E. Spruijt and W. T. S. Huck, *Small*, 2023, **19**, 2303138.

34 K. A. Black, D. Priftis, S. L. Perry, J. Yip, W. Y. Byun and M. Tirrell, *ACS Macro Lett.*, 2014, **3**, 1088–1091.

35 L. Ma, C.-R. Su, S.-Y. Li, S. He, A. Nag and Y. Yuan, *Food Hydrocolloids*, 2023, **144**, 108907.

36 Y. Sun, X. Xu, L. Chen, W. L. Chew, Y. Ping and A. Miserez, *ACS Nano*, 2023, **17**, 16597–16606.

37 E. Hasanvand and S. M. A. Razavi, *Int. Dairy J.*, 2023, **145**, 105716.

38 R. Kembaren, R. Fokkink, A. H. Westphal, M. Kamperman, J. M. Kleijn and J. W. Borst, *Langmuir*, 2020, **36**, 8494–8502.

39 S. S. Nasr, S. Lee, D. Thiyagarajan, A. Boese, B. Loretz and C.-M. Lehr, *Pharmaceutics*, 2021, **13**, 1924.

40 S. S. Nasr, P. Paul, B. Loretz and C.-M. Lehr, *Drug Delivery Transl. Res.*, 2024, **14**, 3339–3353.

41 E. Ban, M. Park, Y. Kim, J. Park and A. Kim, *J. Drug Delivery Sci. Technol.*, 2024, **97**, 105767.

42 J. B. Sabadini, C. L. P. Oliveira and W. Loh, *Langmuir*, 2024, **40**, 2015–2027.

43 T.-Y. Heo, D. J. Audus and S.-H. Choi, *ACS Macro Lett.*, 2023, **12**, 1396–1402.

44 T.-Y. Heo and S.-H. Choi, *J. Phys. Chem. B*, 2024, **128**, 1256–1265.

45 Y. Zhang, Y. Chen, X. Yang, X. He, M. Li, S. Liu, K. Wang, J. Liu and S. Mann, *J. Am. Chem. Soc.*, 2021, **143**, 2866–2874.

46 C.-W. Yeh and Y. Wang, *Macromol. Biosci.*, 2023, **23**, 2200538.

47 X. Meng, S. L. Perry and J. D. Schiffman, *ACS Macro Lett.*, 2017, **6**, 505–511.

48 X. Meng, Y. Du, Y. Liu, E. B. Coughlin, S. L. Perry and J. D. Schiffman, *Macromolecules*, 2021, **54**, 5033–5042.

49 F. Weinbreck, R. H. Tromp and C. G. De Kruif, *Biomacromolecules*, 2004, **5**, 1437–1445.

50 J. Zhang, H. Du, N. Ma, L. Zhong, G. Ma, F. Pei, H. Chen and Q. Hu, *Food Sci. Hum. Wellness*, 2023, **12**, 183–191.

51 X. Zhou, X. Feng, W. Qi, J. Zhang and L. Chen, *Food Hydrocolloids*, 2024, **151**, 109794.

52 H. Liang and J. J. De Pablo, *Macromolecules*, 2022, **55**, 4146–4158.

53 F. Akcay Ogur, S. Mamasoglu, S. L. Perry, F. A. Akin and A. B. Kayitmazer, *J. Phys. Chem. B*, 2024, **128**, 9022–9035.

54 C. Love, J. Steinkühler, D. T. Gonzales, N. Yandrapalli, T. Robinson, R. Dimova and T.-Y. D. Tang, *Angew. Chem., Int. Ed.*, 2020, **132**, 6006–6013.

55 L. Li, B. Lai, J.-N. Yan, M. H. Yambazi, C. Wang and H.-T. Wu, *Food Hydrocolloids*, 2024, **148**, 109445.

56 G. Zhang, Y. Wang, P. Cui, Y. Qiu, S. Ye and A. Zhang, *Process Biochem.*, 2024, **143**, 292–301.

57 T. Lu, K. K. Nakashima and E. Spruijt, *J. Phys. Chem. B*, 2021, **125**, 3080–3091.

58 J. B. Sabadini, C. L. P. Oliveira and W. Loh, *J. Colloid Interface Sci.*, 2025, **678**, 1012–1021.

59 X. Liu, Z. Shi, F. Yu, C. Teng, C. Zhang and Z.-R. Chen, *Aggregate*, 2023, **4**, e363.

60 F. Späth, A. S. Maier, M. Stasi, A. M. Bergmann, K. Halama, M. Wenisch, B. Rieger and J. Boekhoven, *Angew. Chem., Int. Ed.*, 2023, **62**, e202309318.

61 J. Feng, H. Tian, X. Chen, X. Cai, X. Shi and S. Wang, *Food Hydrocolloids*, 2023, **138**, 108439.

62 Q. Hu, H. Lan, Y. Tian, X. Li, M. Wang, J. Zhang, Y. Yu, W. Chen, L. Kong, Y. Guo and Z. Zhang, *J. Controlled Release*, 2024, **365**, 176–192.

63 H. Zhang, J. Vandesompele, K. Braeckmans, S. C. D. Smedt and K. Remaut, *Chem. Soc. Rev.*, 2024, **53**, 317–360.

64 D. Sun, W. Tan, J. Zhao, Y. Tian, S. Li, Z. Zhang, X. Dong, X. Liu, N. Liu, P. Jiao and J. Ma, *Fundam. Res.*, 2024, DOI: 10.1016/j.fmre.2023.11.020.

65 S. Chakraborty, *Sens. Diagn.*, 2024, **3**, 536–561.

66 Y. B. Yu, K. T. Briggs, M. B. Taraban, R. G. Brinson and J. P. Marino, *Pharm. Res.*, 2021, **38**, 3–7.

67 W. C. Blocher and S. L. Perry, *Wiley Interdiscip. Rev.: Nanomed. Nanobiotechnol.*, 2017, **9**, e1442.

68 N. Pippa, M. Karayianni, S. Pispas and C. Demetzos, *Int. J. Pharm.*, 2015, **491**, 136–143.

69 S. P. Moulik, A. K. Rakshit, A. Pan and B. Naskar, *Colloids Interfaces*, 2022, **6**, 45.

70 L.-W. Chang, T. K. Lytle, M. Radhakrishna, J. J. Madinya, J. Vélez, C. E. Sing and S. L. Perry, *Nat. Commun.*, 2017, **8**, 1273.

71 Z. Lin, T. Beneyton, J.-C. Baret and N. Martin, *Small Methods*, 2023, **7**, 2300496.

72 J. E. Laaser, Y. Jiang, S. R. Petersen, T. M. Reineke and T. P. Lodge, *J. Phys. Chem. B*, 2015, **119**, 15919–15928.

73 S. Chuanoi, Y. Anraku, M. Hori, A. Kishimura and K. Kataoka, *Biomacromolecules*, 2014, **15**, 2389–2397.

74 J. J. Madinya, H. Tjo, X. Meng, I. A. Ramírez Marrero, C. E. Sing and S. L. Perry, *Macromolecules*, 2023, **56**, 3973–3988.

75 I. Benavides, W. A. Scott, X. Cai, Z. H. Zhou and T. J. Deming, *Eur. Phys. J. E: Soft Matter Biol. Phys.*, 2023, **46**, 81.

76 A. Hernandez-Garcia, A. H. Velders, M. A. C. Stuart, R. de Vries, J. W. M. van Lent and J. Wang, *Chem. – Eur. J.*, 2017, **23**, 239–243.

77 J. Wang, T. Lu, Y. Li, J. Wang and E. Spruijt, *Adv. Colloid Interface Sci.*, 2023, **318**, 102964.

78 H. J. Kim, B. Yang, T. Y. Park, S. Lim and H. J. Cha, *Soft Matter*, 2017, **13**, 7704–7716.

79 A. D. Slootbeek, M. H. I. van Haren, I. B. A. Smokers and E. Spruijt, *Chem. Commun.*, 2022, **58**, 11183–11200.

80 B. Saini, R. R. Singh, D. Nayak and T. K. Mukherjee, *ACS Appl. Nano Mater.*, 2020, **3**, 5826–5837.

81 I. Bos, E. Brink, L. Michels and J. Sprakel, *Soft Matter*, 2022, **18**, 2012–2027.

82 J. Wang, W. Guan, T. Tan, V. Saggiomo, M. A. C. Stuart and A. H. Velders, *Soft Matter*, 2020, **16**, 2953–2960.

83 G. Sinani, M. E. Durgun, E. Cevher and Y. Özsoy, *Pharmaceutics*, 2023, **15**, 2021.

84 R. Kembaren, J. M. Kleijn, J. W. Borst, M. Kamperman and A. H. Hofman, *Soft Matter*, 2022, **18**, 3052–3062.

85 Y. Zhang, Y. Huang and S. Li, *AAPS PharmSciTech*, 2014, **15**, 862–871.

86 J. R. Magana, C. C. M. Sproncken and I. K. Voets, *Polymers*, 2020, **12**, 1953.

87 C.-G. Wang, N. E. B. Surat'man, J. J. Chang, Z. L. Ong, B. Li, X. Fan, X. J. Loh and Z. Li, *Chem. – Asian J.*, 2022, **17**, e202200604.

88 X. Chen, X. Zhang, S. Yang, J. Wang, T. Tang and M. Gou, *Chin. Chem. Lett.*, 2024, 110021.

89 B. Wu, R. W. Lewis, G. Li, Y. Gao, B. Fan, B. Klemm, J. Huang, J. Wang, M. A. C. Stuart and R. Eelkema, *Chem. Sci.*, 2023, **14**, 1512–1523.

90 S. Deshpande, F. Brandenburg, A. Lau, M. G. F. Last, W. K. Spoelstra, L. Reese, S. Wunnava, M. Dogterom and C. Dekker, *Nat. Commun.*, 2019, **10**, 1800.

91 A. B. Cook, S. Novosedlik and J. C. M. van Hest, *Acc. Mater. Res.*, 2023, **4**, 287–298.

92 Y. Bae and K. Kataoka, *Adv. Drug Delivery Rev.*, 2009, **61**, 768–784.

93 T. D. Vogelaar, A. E. Agger, J. E. Reseland, D. Linke, H. Jenssen and R. Lund, *Biomacromolecules*, 2024, **25**, 4267–4280.

94 C. Yan and W. Zhang, in *Microencapsulation in the Food Industry*, ed. A. G. Gaonkar, N. Vasisht, A. R. Khare and R. Sobel, Academic Press, San Diego, 2014, pp. 125–137.

95 F. M. Menger and B. M. Sykes, *Langmuir*, 1998, **14**, 4131–4137.

96 K. Xiao, Y. Yang, X. Xu, J. E. S. Szymanowski, Y. Zhou, G. E. Sigmon, P. C. Burns and T. Liu, *Inorg. Chem.*, 2024, **63**, 15331–15339.

97 R. Soussi Hachfi, P. Hamon, F. Rousseau, M.-H. Famelart and S. Bouhallab, *Foods*, 2023, **12**, 1040.

98 A. Holkar, S. Gao, K. Villaseñor, M. Lake and S. Srivastava, *Soft Matter*, 2024, **20**, 5060–5070.

99 A. B. Kayitmazer, A. F. Koksal and E. K. Iyilik, *Soft Matter*, 2015, **11**, 8605–8612.

100 G. R. Abraham, A. S. Chaderjian, A. B. N. Nguyen, S. Wilken and O. A. Saleh, *Rep. Prog. Phys.*, 2024, **87**, 066601.

101 P. L. Onuchic, A. N. Milin, I. Alshareedah, A. A. Deniz and P. R. Banerjee, *Sci. Rep.*, 2019, **9**, 12161.

102 M. Abbas, W. P. Lipiński, J. Wang and E. Spruijt, *Chem. Soc. Rev.*, 2021, **50**, 3690–3705.

103 F. Ardestani, A. Haghighi Asl and A. Rafe, *Chem. Biol. Technol. Agric.*, 2022, **9**, 83.

104 J. Reijenga, A. van Hoof, A. van Loon and B. Teunissen, *Anal. Chem. Insights*, 2013, **8**, ACI.S12304.

105 G. Henriksson, A. Englund, G. Johansson and P. Lundahl, *Electrophoresis*, 1995, **16**, 1377–1380.

106 I. G. Darvey, *Biochem. Educ.*, 1995, **23**, 80–82.

107 K. Maslowska-Jarzyna, K. M. Bąk, B. Zawada and M. J. Chmielewski, *Chem. Sci.*, 2022, **13**, 12374–12381.

108 G. Platzer, M. Okon and L. P. McIntosh, *J. Biomol. NMR*, 2014, **60**, 109–129.

109 R. Lunkad, A. Murmiliuk, Z. Tošner, M. Štěpánek and P. Košovan, *Polymers*, 2021, **13**, 214.

110 S. Pahari, L. Sun and E. Alexov, *Database*, 2019, **2019**, baz024.

111 J. N. Aronson, *Biochem. Educ.*, 1983, **11**, 68.

112 Y. Tian, Q. Hu, Z. Sun, Y. Yu, X. Li, T. Tian, X. Bi, Y. Li, B. Niu and Z. Zhang, *Small*, 2024, **20**, 2311890.

113 Y. Sun, S. Y. Lau, Z. W. Lim, S. C. Chang, F. Ghadessy, A. Partridge and A. Miserez, *Nat. Chem.*, 2022, **14**, 274–283.

114 H. Karoui, M. J. Seck and N. Martin, *Chem. Sci.*, 2021, **12**, 2794–2802.

115 J. T. King and A. Shakya, *Biophys. J.*, 2021, **120**, 1139–1149.

116 D. Lachowicz, A. Kaczyńska, A. Bodzon-Kulakowska, A. Karewicz, R. Wirecka, M. Szuwarzyński and S. Zapotoczny, *Int. J. Mol. Sci.*, 2020, **21**, 9664.

117 Q. Zhang, C. Weber, U. S. Schubert and R. Hoogenboom, *Mater. Horiz.*, 2017, **4**, 109–116.

118 N. Deng and W. T. S. Huck, *Angew. Chem., Int. Ed.*, 2017, **56**, 9736–9740.

119 D. E. Bergbreiter, A. J. Mijalis and H. Fu, *J. Chem. Educ.*, 2012, **89**, 675–677.

120 L. Tavares and C. P. Z. Noreña, *Food Measure*, 2022, **16**, 295–306.

121 I. Naassaoui and A. Aschi, *Eur. Biophys. J.*, 2021, **50**, 877–887.

122 A. Veis and C. Aranyi, *J. Phys. Chem.*, 1960, **64**, 1203–1210.

123 S. L. Perry, L. Leon, K. Q. Hoffmann, M. J. Kade, D. Priftis, K. A. Black, D. Wong, R. A. Klein, C. F. Pierce, K. O. Margossian, J. K. Whitmer, J. Qin, J. J. De Pablo and M. Tirrell, *Nat. Commun.*, 2015, **6**, 6052.

124 Y. Chen and W. Ma, *PLoS Comput. Biol.*, 2020, **16**, e1007592.

125 S. F. Ozturk, D. D. Sasselov and J. D. Sutherland, *J. Chem. Phys.*, 2023, **159**, 061102.

126 M. G. Weller, *Life*, 2024, **14**, 341.

127 G. T. M. Bitchagno, V.-A. Nchiozem-Ngnitedem, D. Melchert and S. A. Fobofou, *Nat. Rev. Chem.*, 2022, **6**, 806–822.

128 K. M. Lebold and R. B. Best, *J. Phys. Chem. B*, 2022, **126**, 2407–2419.

129 Y. H. Kim, K. Lee and S. Li, *Chem. Mater.*, 2021, **33**, 7923–7943.

130 Y. Wang, R. Zou, Y. Zhou, Y. Zheng, C. Peng, Y. Liu, H. Tan, Q. Fu and M. Ding, *Chem. Sci.*, 2024, **15**, 13442–13451.

131 E. A. Frankel, P. C. Bevilacqua and C. D. Keating, *Langmuir*, 2016, **32**, 2041–2049.

132 D. Priftis, X. Xia, K. O. Margossian, S. L. Perry, L. Leon, J. Qin, J. J. De Pablo and M. Tirrell, *Macromolecules*, 2014, **47**, 3076–3085.

133 T. Lin, Y. Zhou, Y. Dadmohammadi, M. Yaghoobi, G. Meletharayil, R. Kapoor and A. Abbaspourrad, *Food Hydrocolloids*, 2023, **145**, 109064.

134 J. Zhou, Y. Cai, Y. Wan, B. Wu, J. Liu, X. Zhang, W. Hu, M. A. Cohen Stuart and J. Wang, *J. Colloid Interface Sci.*, 2023, **650**, 2065–2074.

135 W. C. Blocher McTigue and S. L. Perry, *Soft Matter*, 2019, **15**, 3089–3103.

136 W. C. Blocher McTigue and S. L. Perry, *Small*, 2020, **16**, 1907671.

137 R. G. Ingle and W.-J. Fang, *Pharmaceutics*, 2023, **15**, 1158.

138 K. Yadav, K. K. Sahu, Sucheta, S. P. E. Gnanakani, P. Sure, R. Vijayalakshmi, V. D. Sundar, V. Sharma, R. Antil, M. Jha, S. Minz, A. Bagchi and M. Pradhan, *Int. J. Biol. Macromol.*, 2023, **241**, 124582.

139 L. Zhu, J. Luo and K. Ren, *J. Mater. Chem. B*, 2023, **11**, 261–279.

140 M. Lu, H. Xing, A. Zheng, Y. Huang and X.-J. Liang, *Acc. Chem. Res.*, 2023, **56**, 224–236.

141 R. J. Mosley, B. Rucci and M. E. Byrne, *J. Mater. Chem. B*, 2023, **11**, 2078–2094.

142 Z.-G. Lu, J. Shen, J. Yang, J.-W. Wang, R.-C. Zhao, T.-L. Zhang, J. Guo and X. Zhang, *Signal Transduction Targeted Ther.*, 2023, **8**, 1–53.

143 J. R. Vieregg, M. Lueckheide, A. B. Marciel, L. Leon, A. J. Bologna, J. R. Rivera and M. V. Tirrell, *J. Am. Chem. Soc.*, 2018, **140**, 1632–1638.

144 C. Forenzo and J. Larsen, *Mol. Pharmaceutics*, 2023, **20**, 4387–4403.

145 S. M. Naghib, B. Ahmadi, B. Mikaeeli Kangarshahi and M. R. Mozafari, *Int. J. Biol. Macromol.*, 2024, **278**, 134542.

146 L. Ma, X. Fang and C. Wang, *Front. Bioeng. Biotechnol.*, 2023, **10**, 1100365.

147 Z. Wang, X. Zhang, M. Han, X. Jiao, J. Zhou, X. Wang, R. Su, Y. Wang and W. Qi, *J. Mater. Chem. B*, 2023, **11**, 8974–8984.

148 Y. Kakizawa and K. Kataoka, *Adv. Drug Delivery Rev.*, 2002, **54**, 203–222.

149 H. Cabral and K. Kataoka, *J. Controlled Release*, 2014, **190**, 465–476.

150 H. Cho, J. Kim, S. Kim, Y. C. Jung, Y. Wang, B.-J. Kang and K. Kim, *J. Controlled Release*, 2020, **327**, 284–295.

151 H. J. Kim, A. Kim, K. Miyata and K. Kataoka, *Adv. Drug Delivery Rev.*, 2016, **104**, 61–77.

152 S. Abbasi, S. Uchida, K. Toh, T. A. Tockary, A. Dirisala, K. Hayashi, S. Fukushima and K. Kataoka, *J. Controlled Release*, 2021, **332**, 260–268.

153 R. Aman, M. M. Syed, A. Saleh, F. Melliti, S. R. Gundra, Q. Wang, T. Marsic, A. Mahas and M. M. Mahfouz, *Nucleic Acids Res.*, 2024, gkae148.

154 R. A. Kapelner, V. Yeong and A. C. Obermeyer, *Curr. Opin. Colloid Interface Sci.*, 2021, **52**, 101407.

155 P. Kaushik, P. K. Pandey, V. K. Aswal and H. B. Bohidar, *Soft Matter*, 2020, **16**, 9525–9533.

156 X. Zhang, Y. Lin, N. A. Eschmann, H. Zhou, J. N. Rauch, I. Hernandez, E. Guzman, K. S. Kosik and S. Han, *PLoS Biol.*, 2017, **15**, e2002183.

157 P. Chowdhury, B. Saha, K. Bauri, B. S. Sumerlin and P. De, *J. Am. Chem. Soc.*, 2024, **146**, 21664–21676.

158 T. Lu, S. Javed, C. Bonfio and E. Spruijt, *Small Methods*, 2023, **7**, 2300294.

159 A.-G. Niculescu, A. C. Bîrcă and A. M. Grumezescu, *Pharmaceutics*, 2021, **13**, 2053.

160 P. U. Joshi, C. Decker, X. Zeng, A. Sathyavageeswaran, S. L. Perry and C. L. Heldt, *Biomacromolecules*, 2024, **25**(2), 741–753, DOI: **10.1021/acs.biomac.3c00938**.

161 T. Sneideris, N. A. Erkamp, H. Ausserwöger, K. L. Saar, T. J. Welsh, D. Qian, K. Katsuya-Gaviria, M. L. L. Y. Johncock, G. Krainer, A. Borodavka and T. P. J. Knowles, *Nat. Commun.*, 2023, **14**, 7170.

162 M. Peydayesh, S. Kistler, J. Zhou, V. Lutz-Bueno, F. D. Victorelli, A. B. Meneguin, L. Spósito, T. M. Bauab, M. Chorilli and R. Mezzenga, *Nat. Commun.*, 2023, **14**, 1848.

163 K. Roy, H.-Q. Mao, S.-K. Huang and K. W. Leong, *Nat. Med.*, 1999, **5**, 387–391.

164 H. Nishida, Y. Matsumoto, K. Kawana, R. J. Christie, M. Naito, B. S. Kim, K. Toh, H. S. Min, Y. Yi, Y. Matsumoto, H. J. Kim, K. Miyata, A. Taguchi, K. Tomio, A. Yamashita, T. Inoue, H. Nakamura, A. Fujimoto, M. Sato, M. Yoshida, K. Adachi, T. Arimoto, O. Wada-Hiraike, K. Oda, T. Nagamatsu, N. Nishiyama, K. Kataoka, Y. Osuga and T. Fujii, *J. Controlled Release*, 2016, **231**, 29–37.

165 D. Zhou, C. Li, Y. Hu, H. Zhou, J. Chen, Z. Zhang and T. Guo, *J. Mater. Chem.*, 2012, **22**, 10743–10751.

166 A. Herrmann, S. Abbina, N. V. Bathula, P. M. M. Nouri, I. Chafeeva, I. Constantinescu, E. Abbasi, U. Abbasi, M. Drayton, H. D. Luo, H. Moon, A. Gill, Y. Xi, A. K. Bertram, C. Du, R. Haag, A. K. Blakney and J. N. Kizhakkedathu, *Adv. Funct. Mater.*, 2024, **34**, 2406878.

167 W. Liu, J. Deng, S. Song, S. Sethi and A. Walther, *Commun. Chem.*, 2024, **7**, 1–10.

168 C. Delehedde, I. Ciganek, N. Rameix, N. Laroui, C. Gonçalves, L. Even, P. Midoux and C. Pichon, *Int. J. Pharm.*, 2023, **647**, 123531.

169 L. Mott, C. Akers and D. W. Pack, *J. Drug Delivery Sci. Technol.*, 2023, **84**, 104465.

170 C. Salvador, P. Andreozzi, G. Romero, I. Loinaz, D. Dupin and S. E. Moya, *ACS Appl. Bio Mater.*, 2023, **6**, 529–542.

171 Y. Li, B. Humphries, Z. Wang, S. Lang, X. Huang, H. Xiao, Y. Jiang and C. Yang, *ACS Appl. Mater. Interfaces*, 2016, **8**, 30735–30746.

172 Y. Cai, N. Y. Naser, J. Ma and F. Baneyx, *Biomacromolecules*, 2024, **25**, 2390–2398.

173 K. Yoshida, K. Suyama, S. Matsushita, I. Maeda and T. Nose, *J. Pept. Sci.*, 2023, **29**, e3528.

174 R. Leicher, A. Osunsade, G. N. L. Chua, S. C. Faulkner, A. P. Latham, J. W. Watters, T. Nguyen, E. C. Beckwitt, S. Christodoulou-Rubalcava, P. G. Young, B. Zhang, Y. David and S. Liu, *Nat. Struct. Mol. Biol.*, 2022, **29**, 463–471.

175 Y. Zhou, K. Zhang, S. Moreno, A. Temme, B. Voit and D. Appelhans, *Angew. Chem., Int. Ed.*, 2024, **63**, e202407472.

176 S. Cao, T. Ivanov, J. Heuer, C. T. J. Ferguson, K. Landfester and L. Caire Da Silva, *Nat. Commun.*, 2024, **15**, 39.

177 L. Zhang, M. Chen, Z. Wang, M. Zhong, H. Chen, T. Li, L. Wang, Z. Zhao, X.-B. Zhang, G. Ke, Y. Liu and W. Tan, *ACS Cent. Sci.*, 2024, **10**, 1201–1210.

178 W. M. Aumiller, F. Pir Cakmak, B. W. Davis and C. D. Keating, *Langmuir*, 2016, **32**, 10042–10053.

179 A. I. Bhat and G. P. Rao, in *Characterization of Plant Viruses: Methods and Protocols*, ed. A. I. Bhat and G. P. Rao, Springer, US, New York, NY, 2020, pp. 377–381.

180 R. K. Kumar, R. L. Harniman, A. J. Patil and S. Mann, *Chem. Sci.*, 2016, **7**, 5879–5887.

181 S. Gao and S. Srivastava, *ACS Macro Lett.*, 2022, **11**, 902–909.

182 C. E. R. Edwards, K. L. Lakkis, Y. Luo and M. E. Helgeson, *Soft Matter*, 2023, **19**, 8849–8862.

183 V. Lauth, M. Maas and K. Rezwan, *J. Mater. Chem. B*, 2014, **2**, 7725–7731.

184 K. K. Nakashima, A. A. M. André and E. Spruijt, in *Methods in Enzymology*, ed. C. D. Keating, Academic Press, 2021, vol. 646, pp. 353–389.

185 N. S. Heredia, K. Vizuete, M. Flores-Calero, V. K. Pazmiño, F. Pilaquinga, B. Kumar and A. Debut, *PLoS One*, 2022, **17**, e0264825.

186 F. Ardestani, A. Haghighi Asl and A. Rafe, *Chem. Biol. Technol. Agric.*, 2024, **11**, 118.

187 A. Salehi, A. Rezaei, M. S. Damavandi, M. S. Kharazmi and S. M. Jafari, *Food Chem.*, 2023, **405**, 134801.

188 M. H. M. E. van Stevendaal, L. Vasiukas, N. A. Yewdall, A. F. Mason and J. C. M. van Hest, *ACS Appl. Mater. Interfaces*, 2021, **13**, 7879–7889.

189 M. H. van Haren, K. K. Nakashima and E. Spruijt, *J. Syst. Chem.*, 2020, **8**, 107–120.

190 D. L. Rohlfing, *Origins Life Evol. Biospheres*, 1975, **6**, 203–209.

191 X. Mi, W. C. Blocher McTigue, P. U. Joshi, M. K. Bunker, C. L. Heldt and S. L. Perry, *Biomater. Sci.*, 2020, **8**, 7082–7092.

192 H. Chen, Y. Bao, X. Li, F. Chen, R. Sugimura, X. Zeng and J. Xia, *Angew. Chem., Int. Ed.*, 2024, e202410566.

193 J. Li and K. Kataoka, *J. Am. Chem. Soc.*, 2021, **143**, 538–559.

194 K. Koji, N. Yoshinaga, Y. Mochida, T. Hong, T. Miyazaki, K. Kataoka, K. Osada, H. Cabral and S. Uchida, *Biomaterials*, 2020, **261**, 120332.

195 H. Cabral, H. Kinoh and K. Kataoka, *Acc. Chem. Res.*, 2020, **53**, 2765–2776.

196 S. Yousefi Adlsadabad, J. W. Hanrahan and A. Kakkar, *Int. J. Mater. Sci.*, 2024, **25**, 1739.

197 M. Lin, X. Lv, H. Wang, L. Shu, H. Wang, G. Zhang, J. Sun and X. Chen, *Adv. Mater.*, 2024, **36**, 2407378.

198 X. Li, E. K. Dowling, G. Yan, Z. Dereli, B. Bozorgui, P. Imanirad, J. H. Elnaggar, A. Luna, D. G. Menter, P. G. Pilié, T. A. Yap, S. Kopetz, C. Sander and A. Korkut, *Cancer Discovery*, 2022, **12**, 1542–1559.

199 S. K. Yadava, B. P. K. Reddy, M. R. Prausnitz and M. T. Cicerone, *ACS Appl. Mater. Interfaces*, 2024, **16**, 15981–15992.

200 R. Tenchov, J. M. Sasso and Q. A. Zhou, *Bioconjugate Chem.*, 2023, **34**, 941–960.

201 Y. Liu, Y. Huang, G. He, C. Guo, J. Dong and L. Wu, *Int. J. Mol. Sci.*, 2024, **25**, 10166.

202 F. Pir Cakmak, A. T. Grigas and C. D. Keating, *Langmuir*, 2019, **35**, 7830–7840.

203 Y. Qin, L. Ou, L. Zha, Y. Zeng and L. Li, *Mol. Biomed.*, 2023, **4**, 48.

204 Y. Xu, T. Fourniols, Y. Labrak, V. Préat, A. Beloqui and A. des Rieux, *ACS Nano*, 2022, **16**, 7168–7196.

205 R. Kaup, J. B. ten Hove, A. Bunschoten, F. W. B. van Leeuwen and A. H. Velders, *Nanoscale*, 2021, **13**, 15422–15430.

206 A. Pica, I. Russo Krauss, V. Parente, H. Tateishi-Karimata, S. Nagatoishi, K. Tsumoto, N. Sugimoto and F. Sica, *Nucleic Acids Res.*, 2017, **45**, 461–469.

207 E. Kluczka, V. Rinaldo, A. Coutable-Pennarun, C. Stines-Chaumeil, J. L. R. Anderson and N. Martin, *ChemCatChem*, 2024, **16**, e202400558.

208 I. B. A. Smokers, B. S. Visser, A. D. Slootbeek, W. T. S. Huck and E. Spruijt, *Acc. Chem. Res.*, 2024, **57**, 1885–1895.

209 U. Odunze, N. Rustogi, P. Devine, L. Miller, S. Pereira, S. Vashist, H. J. Snijder, D. Corkill, A. Sabirsh, J. Douthwaite, N. Bond and A. Desai, *Nucleic Acids Res.*, 2024, **52**, 9384–9396.

This journal is © The Royal Society of Chemistry 2025